CELSIUS PROJECT THERMAL MODELLING PHASE 1: MODELLING THE HEAT FLOW IN TRANSFORMER SUBSTATIONS

L WRIGHT, J PEARCE

OCTOBER 2017

CELSIUS PROJECT THERMAL MODELLING PHASE 1: MODELLING THE HEAT FLOW IN TRANSFORMER SUBSTATIONS

L Wright, Data Science Group

J Pearce, Temperature & Humidity Group

National Physical Laboratory
Hampton Road, Teddington, Middlesex, TW11 0LW

Approved on behalf of NPL by
Alistair Forbes, Knowledge Leader for the Data Science Department.

CONTENTS

1   INTRODUCTION

This report is a deliverable of Phase 1 of the thermal flow study that forms NPL's contribution to the Celsius project. The Celsius project aims to use measurement and modelling to assess the thermal performance of assets, including substations and the transformers inside them. This assessment will enable network managers to ensure their infrastructure is able to meet future anticipated rises in demand without thermal damage occurring. The models reported here focus on cooling of transformers that are situated within buildings.

The report includes:

- A thorough literature survey to establish best practice for thermal modelling of substation buildings in the industry, and to avoid duplication of existing developments where possible.
- Description of a set of thermal models using the multi-physics finite element software Comsol Multiphysics™ which can express the relevant phenomena (conductive, convective, and radiative heat transfer, and air flow) in terms of differential equations.
- Demonstration of the validation of this approach by comparing model results to experimental temperature measurements supplied by Electricity North West.
- Use of the model results to develop recommendations for the ventilation arrangements in both new-build and retrofit scenarios.

This report includes a summary of the literature survey (section 2), a full specification of the Comsol model (section 3), investigations of some of the assumptions made during the modelling (section 4), a detailed discussion of the results of the various models run (section 5), and recommendations for alterations to ventilation (section 6).

The aim of the models described here is twofold. The principal aim is to demonstrate that coupled fluid dynamics and thermal models can be used to simulate the air flow and temperature distribution within substations. The models use measured data gathered at specific substations as input conditions and predict temperatures at other measured points, and if the agreement between model results and measured values is sufficiently good, and any discrepancies are explicable, then the approach is acceptable. The models are of specific buildings at specific times and do not consider the effects of increased heating due to extra loading, solar gain, or other heat sources. Phase 2 of the work will study these aspects in more depth, and may lead to revision of the recommendations made here.

A second aim is to use the model results to look at the effects of vent placement and size on the airflow and temperature distribution within the substation in order to provide advice on these aspects for new-build substations and for the retrofit of old substations.

2   LITERATURE SURVEY

A literature review has been carried out with two aims:

1.   To identify the current state of the art of modelling heat transfer in substation buildings.
2.   To identify sources of information to support development of a model for the heat transfer in the specific cases of interest to Electricity North West.

The information required for model development includes thermal properties for the likely materials of the substation building, assessment of turbulence models, and ways of modelling air flow in enclosed spaces with significant heat sources.

Web Of Science is a search tool that accesses databases of scientific literature across decades and is arguably the primary tool for scientific literature surveys. All Web Of Science searches mentioned were carried out on 3rd April 2017. Other papers have been identified through more general web searches.

2.1 AIM 1: STATE OF THE ART MODELS OF HEAT TRANSFER IN SUBSTATION BUILDINGS

A search for papers on Web of Science for substation thermal models brought up 114 papers. Many of these were models of heating networks or of the details of heat transfer within individual components such as connectors and behaviour such as arcing. Some were detailed models of oil flow and heat transfer within transformers but these were not regarded as directly relevant to this project. The papers that are of direct relevance to this project can be split into two broad classes: zonal models and detailed flow models.

Zonal models (the term is common throughout the literature on thermal modelling of buildings) are lumped parameter models that assign a capacitance to each component in the system that can store heat, a fixed temperature to components whose temperature is known, and a conductivity (possibly temperature-dependent) to each exchange of heat between two system components. The models effectively assume that a given component is at a single uniform (but time-varying) temperature, and that heat transfer is determined by this averaged component temperature.

These models are good at predicting time-dependent behaviour of a complete system, but determination of the input parameters is only possible by data fitting which means that determined values may not be transferrable from one system to another, and since changes such as altering the cooling system would affect these parameters in an unpredictable manner, the models are not really suitable for the first stage of this project. Summaries of the most relevant zonal model papers are given [1-7] below.

Detailed flow modelling of substations typically involves the use of computational fluid dynamics (CFD) to calculate the air flow regime and ensuing temperature distribution inside a substation building. This is the approach used by NPL in this project. The technique is suitable for predicting "snapshots" of steady-state behaviour, but is often too computationally expensive to be used for prediction of long-term behaviour. Hence it is a suitable tool for examining the impact of a change in ventilation on the energy removed from a building in the steady state, but will not be used to predict (for instance) how long it will take an overheated transformer to cool down in the initial phase of the project.

Eventually it may be possible to use a detailed flow model to evaluate the input parameters required for a zonal model so that the long-term behaviour of the original system can be compared to the long-term behaviour of a system with altered ventilation. This approach has been taken for underground substations in [8-9].

The following papers were identified as being directly relevant to this project:

[1] "Non-stationary thermal model of indoor transformer stations", Radakovic, Z, and Maksimovic, S. Electrical Engineering 84, 109-117, 2002.

Paper combines existing models of heat transfer between windings and oil and oil and air, and a model based on "the Hoppner formula" linking power loss through natural ventilation (a search for this only yields the references above) with standard approaches to modelling heat transfer through walls, ceiling and door. Where possible parameters were determined directly from measurements of the transformer, but some were derived by fitting the model to temperature monitoring data.

[2] "Nonlinear thermal modelling of indoor and outdoor oil-immersed power transformers", Iskender, I, and Mamizadeh, A. Journal of Electrical Engineering, 60(6), 321-327, 2009.
[3] "Evaluation of permissible loading for indoor oil-immersed distribution transformers", Mamizadeh, A, and Iskender, I. Electrical and Electronics Engineering, 10.1109/ELECO.2009.5355332, 2009.
[4] "An improved nonlinear thermal model for MV/LV prefabricated oil-immersed power transformer substations", Iskender, I and Mamizadeh, A. Electrical Engineering, 93(1), 9-22, 2011.
[5] "Analyzing and comparing the hot-spot thermal models of HV/LV prefabricated and outdoor oil-immersed power transformers", Mamizadeh, A, and Iskender, I. International Journal of Electrical, Computer, Energetic, Electronic and Communication Engineering, 6(1), 2012.
[6] "Evaluation and comparing the loss of life for outdoor and MV/LV prefabricated oil immersed power transformer based on nonlinear thermal models", Mamizadeh, A, and Iskender, I. Electrical and Electronics Engineering, 2011. From http://ieeexplore.ieee.org/document/6140218/

The authors derive a zonal model of heat transfer for indoor and outdoor transformers and apply it in various situations. [2] derives the full model, including detailed expressions for heat transfer within the oil. [3] applies the model to estimate maximum safe load given the ambient temperature. [4] introduces a more complicated model of the heat transfer within the building that includes ventilation. [5] develops a model for the hot-spot temperature within the transformer, and [6] uses that model to estimate the aging of insulation, and associated loss of lifetime, due to hot spot temperature.

[7] "Dynamic Thermal Modeling of MV/LV Prefabricated Substations", Degefa, M Z, Millar R J, Lehtonen M and Hyvönen, P. IEEE Transactions on Power Delivery, 29(2), 786-793, 2014.

Zonal model with more focus on the effects of environment and less on the oil behaviour. Includes radiative exchange, and uses an expression for natural ventilation based on some approximate consideration of fluid flow.

[8] "Numerical modelling of the natural ventilation of underground transformer substations", Ramos, JC, Beiza, M, Gastelurrutia, J, Rivas, A, Anton, R, Larraona, GS, de Miguel, I. Applied Thermal Engineering, 51(1-2), 852-863, DOI: 10.1016/j.applthermaleng.2012.10.032, 2013.
[9] "Zonal thermal model of the ventilation of underground transformer substations: Development and parametric study", Beiza, M; Ramos, JC; Rivas, A; Anton, R; Larraona, GS; Gastelurrutia, J; de Miguel, I. Applied Thermal Engineering, 62(1), 215-228, DOI: 10.1016/j.applthermaleng.2013.09.032, 2014.

These papers present the development of a zonal model of two designs of underground substation [9] with parameters derived from the results of a full flow model of those designs [8]. The zonal model is a steady-state model including mass flow and heat transfer and so is more complicated than those in references [1-7] that only consider heat transfer. In addition, the zonal model divides the full space into more zones than the models in [1-7], so that variations of temperature and air velocity can be captured more accurately. As a result an iterative method is required to solve the model. The full flow model is described in full in [8], and there are a number of points that could be taken up in NPL's full flow model, specifically:

- air is modelled with the ideal gas equation,
- the Re-Normalisation Group (RNG)[1] k-ϵ turbulence model with a one-equation model by Wolfstein near walls is used as it gives good agreement with measurements (additionally turbulence boundary conditions and inlet conditions can be carried straight over),
- details of grille and grating geometries are included as they affect airflow direction
- walls are treated with 1-D heat transfer and with radiation and convection on the external surface,
- no slip conditions and smooth walls for fluid boundary conditions,
- temperature measurements on the transformer are mapped to the model as thermal boundary conditions,
- internal radiative exchange is included.

[10] "Flow and heat distribution analysis of different transformer sub-stations", Hasini, H, Shuaib, N H, Yogendran, S B, Toh, K B. IOP Conference series: Materials Science & Engineering 50, 012044, 2013.

Full CFD model of flow within three geometries of ventilated substation using the k-ϵ turbulence model. No material properties are given and few details of boundary conditions are supplied other than in general terms.

2.2 AIM 2: INFORMATION TO SUPPORT MODEL DEVELOPMENT

Two classes of information have been sought: information that will generally support development of the model, and information about parameter values (such as thermal properties of building materials) that will be entered into the model.

A search on Web Of Science for "ventilation building model" as a topic identifies almost 4,000 papers, mostly zonal models, and adding CFD to the search terms brings the total down to 827. The majority of these papers focussed on ventilation of inhabited or livestock buildings or flow between buildings. Many papers are focussed on pollutant concentrations or thermal comfort. The key difference between these situations and our problem of interest is the presence of a strong heat source inside the substation building. The titles of the papers were scanned to check for any papers handling this type of situation, and several of possible relevance were identified. These papers are summarised below.

[11] "Computational simulations and optimization of flow and temperature distributions in a large-scale power plant building", Lee, T, Singh, H, Lee, J, Jeong, H-M, and Sturm, D. Building Simulation, 4(4), 341-349, 2011.

Reports a CFD model of the inside of a power station. Boilers and turbines are regarded as fixed-flux regions, with the flux being estimated by running repeatedly with different values and choosing the values that agreed best with temperature measurements. The RNG k-ϵ model is used for turbulence. Losses through walls (and presumably ceilings) are treated as linear with a known coefficient: it is not entirely clear whether the model treats wall temperature and air temperature as two distinct entities or not. The initial model is validated against temperature measurements and various ventilation approaches are compared using the model.

[12] "Computational investigation of ventilation effectiveness in a paper producing industry", Markatos, N C. Drying Technology, 18(9), 2051-2064, 2000.

---

1 Yakhot, V., Orszag, S.A., Thangam, S., Gatski, T.B. & Speziale, C.G. (1992), "Development of turbulence models for shear flows by a double expansion technique", Physics of Fluids A, Vol. 4, No. 7, pp1510-1520.

Reports a fairly crude model of heat, mass and moisture transport in a paper factory. Heat sources appear to be treated as fixed flux conditions. Ventilation is assumed to have known inlet velocities. Heat losses through the walls are neglected.

[13] "Numerical and experimental study of 3D turbulent airflow in a full scale heated ventilated room", Lariani, A, Nesredding, H, Galanis, N. Engineering Applications of Computational Fluid Dynamics, 3(1), 1-14, 2014. Electronic copy not available.

Reports results of simulation and measurement of air flow in a room with an electric heater and forced ventilation. The introduction contains a short summary of the literature on modelling similar situations, all suggesting that the k-ε turbulence model is a good choice for modelling situations involving both natural and forced convection. The model is validated against measurements of temperature and air velocity and shows good agreement in all cases. The validated model is used to assess the effects of moving the outlet vent.

As has been mentioned elsewhere, the model will be built using the Comsol finite element package. A further source of information about modelling air flow in buildings is a worked example in the Comsol library called "Displacement Ventilation". This model assumes that the air velocity at the inlet is known, so the circumstances are slightly different, but the worked example offers various tips to improve convergence such as extending inlets and outlets slightly to avoid problems with velocity conditions. The model uses the k-ω turbulence model, believed to be better for jet spreading problems, but it is not expected that jet spreading is of relevance to our case so the k-ϵ model will be used instead (as this is more common in the relevant literature). The two models use different forms to describe the rate of dissipation of the turbulent kinetic energy, with the k-ω model being more commonly used where interaction between the fluid and a wall is a key dissipation mechanism. Some guidance on boundary condition options may also be taken from this model.

The models reported here treat the heat losses through the walls and ceiling as a boundary condition rather than including details of the wall structure in the model directly. The full mathematical formulation of this condition is given in section 3.4.1 of this document. Implementation of the condition requires thermal properties of the walls and roof. Thermal properties of building materials are commonly characterised as a U-value, units W m^{-2} K^{-1}, defined as [thermal conductivity]/[thickness]. In some cases the U-value[2] characterises a complete structure (e.g. a cavity wall with insulation) and is an effective figure for that structure. Some references give effective thermal conductivities rather than U-values. In all cases, the values will relate to a structure of specific dimensions (e.g. cavity width, insulation thickness, etc.) which should be taken into account when identifying the correct value.

NPL has a long history of research into accurate measurement of U-values. Much of the work has focussed on development of measurement standards, but some reports [14, 15, 16] include values for specific materials and structures that are relevant to this project. The Buildings Research Establishment (BRE) has various documents related to thermal properties of structures. One useful source is the document "Solid wall heat losses and the potential for saving energy. Literature review" [17] which contains a table of some typical values from the literature. There are several guidance documents published by government [18], local authority building controls [19] and heritage organisations [20] that contain typical values for a variety of structures.

NPL considers that the most comprehensive, and accurate, values can be obtained from [21] the Chartered Institution of Building Services Engineers (CIBSE) GVA/15 CIBSE Guide A: Environmental Design. Unless stated otherwise, this has been used as a primary source for material properties.

---

2 https://en.wikipedia.org/wiki/Thermal_transmittance

3 MODEL DEFINITION

The aim of the model is to compare different arrangements for cooling of substation buildings. The cooling that occurs will depend on the temperature of the transformer, the ambient temperature, the building structure, and the arrangement of vents and other cooling devices.

3.1 NOTATION

This section defines the symbols and notation used repeatedly in definition of the models. Bold type is used to indicate a vector quantity, and $f(\mathbf{x})$ means that f is a function of the quantity $\mathbf{x}$.

Quantity	Symbol	Unit
Air temperature	$T(\mathbf{x}, t)$	K
Position within the building	$\mathbf{x}$	m
Time	t	s
Air pressure	p	Pa
Air density	$\rho(p, T)$	kg m^{-3}
Air specific heat capacity	c_p	J kg^{-1} K^{-1}
Air velocity	$\mathbf{u}$	m s^{-1}
Air dynamic viscosity	μ	Pa s
Air thermal conductivity	λ	W m^{-1} K^{-1}
Temperature of walls/ceiling inside the building	$T_{\text{in}}(\mathbf{x})$	K
Temperature of walls/ceiling outside the building	$T_{\text{out}}(\mathbf{x})$	K
External air temperature	T_{amb}	K
Acceleration due to gravity	g	m s^{-2}
Thermal expansion coefficient of air	β	K^{-1}
Heat transfer coefficient (various suffices)	h	W m^{-2} K^{-1}
Heat flux (various suffices)	Q	W m^{-2}
Turbulent dissipation	ϵ	m^2 s^{-3}
Turbulent kinetic energy	k	m^2 s^{-2}

3.2 DETAILS OF BUILDINGS AND DATA COLLECTION TIMINGS

Six different real-world buildings have been modelled in detail. Four were brick buildings and two were glass fibre reinforced plastic (GFRP). The site name, construction material, and approximate internal dimensions (length by width by height) of each building are listed in table 1. Each of the actual buildings has been fitted with a number of temperature sensors. Some sensors are used to inform boundary conditions within the model, and some are used to provide validation data to compare with the model results.

To facilitate the accurate construction of the model geometry, a wide range of dimensional measurements were made within each building to define the size and location of all features that might affect the airflow. These features included vents, switchgear, and the transformer. Extensive photographs of each location were also taken, providing further information about location and orientation of each object. Objects such as switchgear etc have been modelled as cuboids that affect

the airflow: their thermal behaviour has not been considered. The effects of this assumption are discussed in section 4.5.

Table 1: Summary of substations modelled.

Location name	Construction material	Dimensions (LxWxH, m)
Acorn Street	Brick	6.44 x 3.60 x 3.10
Emmanuel Street	Brick	6.88 x 5.00 x 4.30
Portland Grove	Brick	6.45 x 3.86 x 3.20
Southgate Industrial Estate	GFRP	3.64 x 3.05 x 2.50
Town Bridge	GFRP	3.27 x 2.97 x 2.50
Wentworth Road	Brick	6.15 x 3.89 x 2.87

It has been assumed that the only significant air flow occurs through the vents, so any leaks under doors etc. are neglected. Conversely it has been assumed that all vents are clear and unblocked. The effects of the latter assumption have been assessed in section 4.4.

The GFRP structures have GFRP walls and GFRP roofs. Measurements taken on site suggest that the GFRP is about 25 mm thick in all regions. Similarly, the walls of the brick buildings are all approximately 275 mm thick. The only information available about roof construction of brick buildings is the photographs taken at the various sites. These photographs suggest that all of the chosen sites have near-flat roofs with tar paper outer layers and wood panels beneath, but some may have additional cement. In all cases (brick and GFRP) the roofs were taken to be flat because the small changes in height that were measured are unlikely to affect the airflow.

The main source of information about vent geometry is similarly photographic. Many of the vents are metal louvred constructions. Dimensions of the louvres and the spacing have been estimated from the photographs throughout, and the louvre angle has been assumed to be 45 degrees in all cases. Two buildings have air bricks[3] for ventilation. In these cases a similar air brick [24] has been identified on a builders' merchant website and the dimensions and air hole size have been measured from the image on that site. Both GFRP buildings have vents at floor level, in one case louvred vents and in the other a gap with an angled baffle, and an overlapping wall at roof level to allow air flow without allowing rain to enter. Both baffled structures are sketched in figure 1.

The logged data for each building from December 2016 to March 2017 was examined. For each building, the time that showed the largest difference between air inlet temperature and top oil temperature was selected for the initial validation, since these situations show the largest amount of heat to be removed from the transformer and hence represent the most critical situations.

---

3 A brick-sized block with holes which is embedded in a wall to allow ventilation through it.
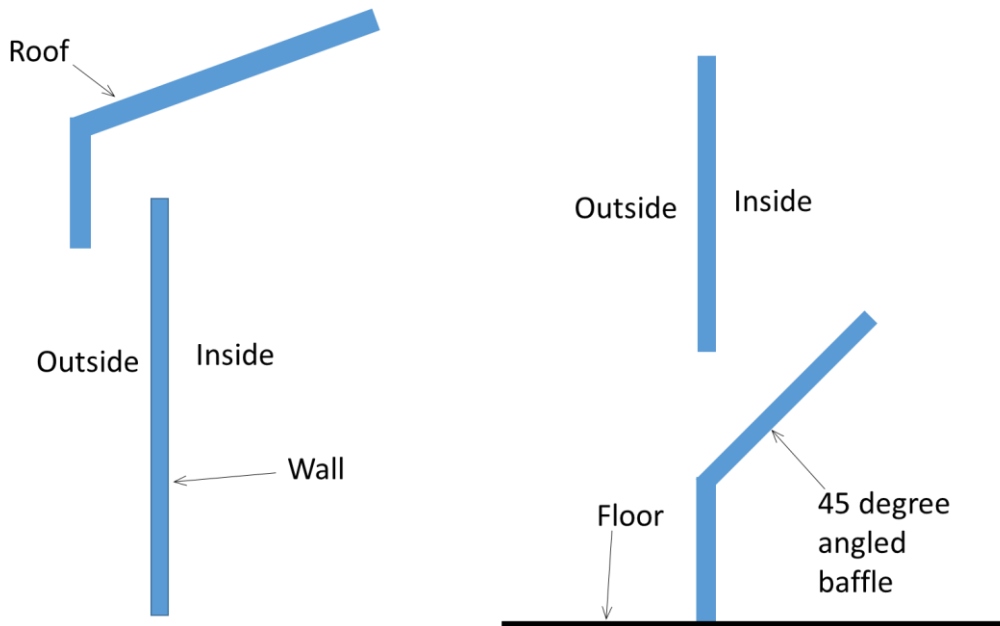
Figure 1: Baffled wall structures used in the GFRP buildings

3.3 WALL AND ROOF MATERIAL PROPERTIES

Determination of the heat transfer through the walls requires knowledge of wall thickness and of the thermal conductivity of the wall materials. Two wall materials have been considered: brick and glass fibre reinforced plastic (GFRP). The mortar in the walls is neglected.

The thermal conductivity of GFRP is dependent on the percentage of glass fibre in the composite. Manufacturer's websites [22, 23] suggest a thermal conductivity of between 0.2 W m^{-1} K^{-1} and 0.35 W m^{-1} K^{-1}. A value of 0.275 W m^{-1} K^{-1} has therefore been used as the mid-point of the range.

The thermal properties of brick have been taken from the CIBSE Guide A Environmental Design [21]. Section 3.5.5 of this document discusses the thermal properties of masonry materials and provides a set of values for standard moisture content conditions for a range of brick densities in table 3.1. Since the brick density is unknown, the median value of 1600 kg m^{-3} has been assumed, leading to a thermal conductivity of 0.71 W m^{-1} K^{-1} for exposed (i.e. externally facing) brickwork.

The Electricity North West document ES352 I6 governing design of distribution substations and transforming points requires that the maximum U-value for the roof of a substation is 1.13 W m^{-2} K^{-1}, so in the absence of any other information this value has been used for roofs of brick buildings.

3.4 MODEL DETAILS

3.4.1   Governing equations

The model describes the airflow with the temperature-dependent Navier-Stokes equations and initially, following the guidance in the literature survey above, the k-ϵ turbulence model (k is the turbulent kinetic energy and ϵ is the turbulent dissipation). Steady-state solutions of the equations have been sought as it is expected that the time scale of changes in the air flow will be over a much shorter time scale than the changes to the temperature of the transformer, making the model quasi-static.

Using the notation defined in section 3.1, the full set of equations describing the system is:

$$\nabla.\left(\rho\mathbf{u}\right) = 0 \tag{1}$$

$$\rho \mathbf{u} \nabla \cdot (\mathbf{u}) = \nabla \cdot \left(-p\mathbf{I} + (\mu + \mu\mu_T)(\nabla\mathbf{u} + (\nabla\mathbf{u})^T) - \frac{2}{3}(\mu + \mu\mu_T)(\nabla \cdot \mathbf{u})\mathbf{I} - \frac{2}{3}\rho k\mathbf{I} \right) \tag{2}$$
$$- g\rho\mathbf{e}_z$$

$$\rho c_p(\mathbf{u}\cdot\nabla T) = -\nabla \cdot (\lambda\nabla T) \tag{3}$$

$$\rho(\mathbf{u}\cdot\nabla)k = \nabla \cdot \left[\left(\mu + \frac{\mu_T}{\sigma_k} \right)\nabla k \right] + P_k - \rho\epsilon \tag{4}$$

$$\rho(\mathbf{u}\cdot\nabla)\epsilon = \nabla \cdot \left[\left(\mu + \frac{\mu_T}{\sigma_\epsilon} \right)\nabla\epsilon \right] + C_{\epsilon 1}\frac{\epsilon}{k}P_k - C_{\epsilon 2}\rho\frac{\epsilon^2}{k} \tag{5}$$

where

$$\mu_T = \rho C_\mu \frac{k^2}{\epsilon} \tag{6}$$

$$P_k = \mu_T \left[\nabla\mathbf{u}:(\nabla\mathbf{u} + (\nabla\mathbf{u})^T) - \frac{2}{3}(\nabla \cdot \mathbf{u})^2 \right] - \frac{2}{3}\rho k\nabla \cdot \mathbf{u} \tag{7}$$

The values of the constants used in the turbulence equations have, according to Wikipedia, been obtained by data fitting to a variety of turbulent flows and the generally accepted values (all dimensionless) are

$$C_\mu = 0.09,\ \sigma_k = 1.00,\ \sigma_\epsilon = 1.30,\ C_{\epsilon 1} = 1.44,\ C_{\epsilon 2} = 1.92.$$

This version of the equations assumes that the work done by pressure changes and the viscous heating can both be neglected. For air flows at near room temperature and near standard pressure, this is a reasonable assumption.

3.4.2   Air properties

The air density has been modelled as a function of temperature and pressure directly rather than using the Boussinesq approximation for buoyant flows, so the dependence is given by

$$\rho = \frac{p}{287\,T} \tag{8}$$

where the value 287 J kg^{-1} K^{-1} is the specific gas constant for dry air and this expression has been obtained by assuming air to be an ideal gas. The air is assumed to be dry throughout. It is expected that the pressure fluctuations will be sufficiently small that the density will effectively be a function of temperature only, but this is not enforced directly. The other material properties of the air are modelled using the inbuilt temperature-dependent functions of Comsol, given by:

$$\lambda = -2.28 \times 10^{-3} + 1.15 \times 10^{-4}T - 7.90 \times 10^{-8}T^2 \tag{9}$$
$$+ 4.12 \times 10^{-11}T^3 - 7.44 \times 10^{-15}T^4$$

$$\mu = -8.38 \times 10^{-7} + 8.36 \times 10^{-8}T - 7.69 \times 10^{-11}T^2 \tag{10}$$
$$+ 4.64 \times 10^{-14}T^3 - 1.07 \times 10^{-17}T^4$$

$$c_p = 1050 - 0.373T + 9.45 \times 10^{-4}T^2 - 6.02 \times 10^{-7}T^3 + 1.29 \times 10^{-10}T^4 \tag{11}$$

3.4.3   Boundary conditions and heat fluxes

The heat flux due to convective heat transfer from a surface to air can be described by the equation

$$Q = h(T_s - T) \tag{12}$$

where Q is the heat flux in W m^{-2} and is positive if energy is added to the air, T_s is the temperature of the surface, T is the air temperature, and h is a heat transfer coefficient.

The heat transfer coefficient for a flow past an object depends on various aspects of the fluid material properties and the flow geometry. These features are captured in the dimensionless quantities the Rayleigh number (Ra) and Prandtl number (Pr), where

$$\text{Ra} = \frac{g\beta c_p \rho^2}{\mu\lambda}|T_s - T_\infty|L^3 \tag{13}$$

$$\text{Pr} = \frac{c_p \mu}{\lambda} \tag{14}$$

where L is a typical length scale (i.e. length of cooling fins), β is the thermal expansion coefficient of the gas ($= 1/T$ for air as an ideal gas), g is acceleration due to gravity, T_∞ is the fluid temperature far from the surface, and all material properties should be evaluated at $(T_s + T_\infty)/2$.

For unforced flow past a vertical plate (where unforced means that the fluid velocity is due to buoyancy rather than a fan or similar driving force), a widely-used expression for the heat transfer coefficient is given by

$$h = \frac{\lambda}{L}\left(0.825 + \frac{0.387\,\text{Ra}^{1/6}}{(1 + [0.492/\text{Pr}]^{9/16})^{8/27}}\right)^2 \tag{15}$$

This quantity was evaluated for a range of surface temperatures before using it in the model to see how sensitive the value is to inputs. The results of these calculations are reported below in section 3.4.6.

Throughout the following, "walls" is used to mean walls, floor, or ceiling. Heat flow vertically in the walls will be assumed to be insignificant compared to heat flow through the walls, which is reasonable as the walls are much thinner than they are tall and the most significant temperature difference is across their thickness.

The heat transfer through the walls, ceiling and floor has several components. The outer surface of the building will lose heat to the atmosphere, and this process is described by an equation of the form (12) where the ambient temperature replaces the fluid temperature, and may gain energy if solar radiation occurs. Solar radiation will be characterised using a single heat flux value Q_S applied uniformly over an area of the building and re-radiation from the surface to the air temperature if necessary. The inner surface of the wall will exchange heat with the air in the building, the process being described by equation (12). The heat transfer from one side of the wall to the other will depend on the structure of the wall through an equation of the form

$$Q = U_w(T_{\text{in}} - T_{\text{out}}) \tag{16}$$

where Q is the heat flux through the wall (positive is heat leaving the building) in W m^{-2}, U_w is an effective heat transfer coefficient for the wall in W m^{-2} K^{-1} that takes wall thickness and structure into account, known as the U-value, T_{in} is the temperature of the wall inside the building, and T_{out} is the temperature of the outside of the building. The literature search above has listed some sources of U-values. For a uniform material of thickness h_0 and thermal conductivity λ_w, $U_w = \lambda_w/h_0$.

For the material properties and wall thicknesses listed in sections 3.2 and 3.3, the U-value of a brick wall is approximately 2.6 W m^{-2} K^{-1}, and that of a GFRP structure is about 11 W m^{-2} K^{-1}. These values mean that for a fixed temperature difference across a wall, energy flows through the GFRP wall about 5 times faster than it does through brick. This increase is largely due to the GFRP wall being thinner.

There are two distinct cases of boundary condition that could be considered, describing two distinct physical cases. In the first case, the complete building system is in equilibrium with the outside world, i.e. the wall temperature has responded to the change in external temperature quickly (i.e. at the same rate as the external temperature is changing). This case would occur when the outside temperature is only changing slowly, or when the building has low thermal mass, i.e. the product of its density and its specific heat capacity is low so that it does not store energy in its walls. In the second case, the external wall temperature is not in equilibrium with the outside world and is only losing heat to the outside world slowly, so the outside wall temperature should be regarded as fixed. This situation could occur if a building with a high thermal mass has been heated over a long period. Both of these conditions can be reduced to an expression similar to equation (12). The full derivation for these expressions is given in section 3.4.5. The model has assumed that the buildings have a sufficiently low thermal mass that equilibrium occurs over the time period of interest. This assumption is tested in section 4.1.

The vents in the walls will be treated as allowing the air to enter or exit, depending on the local pressure value. The external air is assumed to be at atmospheric pressure, taking elevation into account, and at the temperature measured at the inlet vent of the building. Vent geometries are modelled in detail to capture the correct flow. The velocity of the air as it enters or leaves will be determined by Comsol from the pressure difference rather than being driven.

3.4.4   Heat sources

The main source of energy coming into the building is the transformer. The transformer will be regarded as having a fixed temperature distribution, determined from interpolation of the temperature sensor measurements, and as transferring energy to the air through free convection. The transformer has a set of cooling fins that increase the area available for heat loss. These fins would be challenging to model in detail, but the amount of energy they put into the air can be modelled more simply.

The fins have two effects on the airflow. The first is that the airflow past the fins is predominantly vertical. The second is that the air that flows past the fins will get hotter. The energy transfer is proportional to the surface area of the fins and to the temperature difference between the fins and the air, as described above. An equivalent transfer of energy can be modelled by treating the volume containing the fins as a volume source of energy. The effects of the fins on the direction of airflow can be approximated by including walls at each end of this volume so that the flow through the volume is mostly vertical. This approach is much more computationally efficient than a complete model of the transformer as the fine details of the fins need not be included.

Suppose that a fin has total surface area A and that the volume enclosing the fins is V. For N such fins, the total area is therefore NA. Hence if a volumetric heat source is defined in a way equivalent to equation (12), then the volumetric heat transfer coefficient $\hat{h}$ must be such that

$$NAh = V\hat{h} \qquad\qquad (17)$$
$$\Rightarrow \hat{h} = NAh/LV$$

in order that the correct amount of energy is transferred to the air. For rectangular fins this expression can be simplified but for tubular fins it is best left in this form. A small-scale test model has been created to compare this approach to a detailed fin model to assess the effects of the approximation. The results of this test model are reported in section 4.2 below.

The transformer (main body and fins) is treated as being a source of heat, but not as a source of air (i.e. mass flow). This approach is reasonable because the expelling of air when expansion of the oil occurs is a short-term event, but the outer casing of the transformer will remain at an elevated temperature over a longer timescale.

3.4.5   Derivation of the boundary conditions for thermal transfer through a wall or roof

The derivation of the form of the boundary conditions is based on two assumptions: linearity of temperature within the wall, and continuity of heat flux. Linearity of temperature within the wall is reasonable for a steady-state situation neglecting conduction within the wall and considering the wall to have a uniform U-value. Continuity of heat flux is a consequence of conservation of energy.
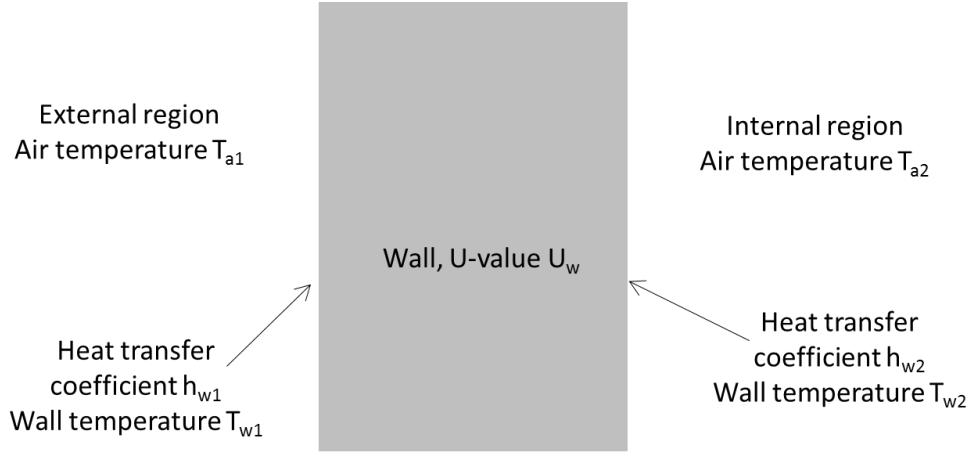

Figure 2: Notation used in the derivation of the boundary condition.

Consider the situation in figure 2. The two equations defining continuity of heat flux at the wall boundaries are

$$Q_{w1} = h_{w1}(T_{a1} - T_{w1}) = U_w(T_{w1} - T_{w2}) \tag{18}$$

$$Q_{w2} = h_{w2}(T_{a2} - T_{w2}) = U_w(T_{w2} - T_{w1}) \tag{19}$$

where for the first type of boundary condition T_{a1}, h_{w1}, U_w, h_{w2} are known, T_{w1} and T_{w2} are unknown, and the aim is to write Q_{w2} (the heat flux between the internal air and the wall, positive if the energy goes from the air into the wall) as a function of T_{a2} and known quantities. For the second type, T_{w1} is known and T_{w2} is not, and the aim remains the same.

Rearranging (18) for T_{w1} gives

$$T_{w1} = \frac{h_{w1}T_{a1}}{(U_w + h_{w1})} + \frac{T_{w2}U_w}{(U_w + h_{w1})} \tag{20}$$

and substituting into (19) and rearranging for T_{w2} gives

$$T_{w2} = \left[\frac{U_w + h_{w1}}{h_{w1}U_w + h_{w2}U_w + h_{w1}h_{w2}}\right]\left\{h_{w2}T_{a2} + \frac{U_w h_{w1}T_{a1}}{(U_w + h_{w1})}\right\} \tag{21}$$

so that the required expression for the heat flux is

$$Q_{w2} = \frac{h_{w2}h_{w1}U_w}{h_{w1}U_w + h_{w2}U_w + h_{w1}h_{w2}}(T_{a2} - T_{a1}). \tag{22}$$

If T_{w1} is regarded as known, (19) is rearranged and substituted in to give

$$T_{w2} = \frac{h_{w2}T_{a2} + T_{w1}U_w}{(U_w + h_{w2})} \tag{23}$$

$$Q_{w2} = \frac{h_{w2}U_w}{(U_w + h_{w2})}(T_{a2} - T_{w1}). \tag{24}$$

These expressions are implemented directly in the model as convection conditions.

3.4.6   Heat transfer coefficient variation

Equations (9) to (15) were used to calculate the heat transfer coefficient and associated heat flux for a physically reasonable range of surface and air temperatures. Figure 3 shows the calculated heat transfer coefficients plotted against surface temperature, with each line representing a different air temperature.
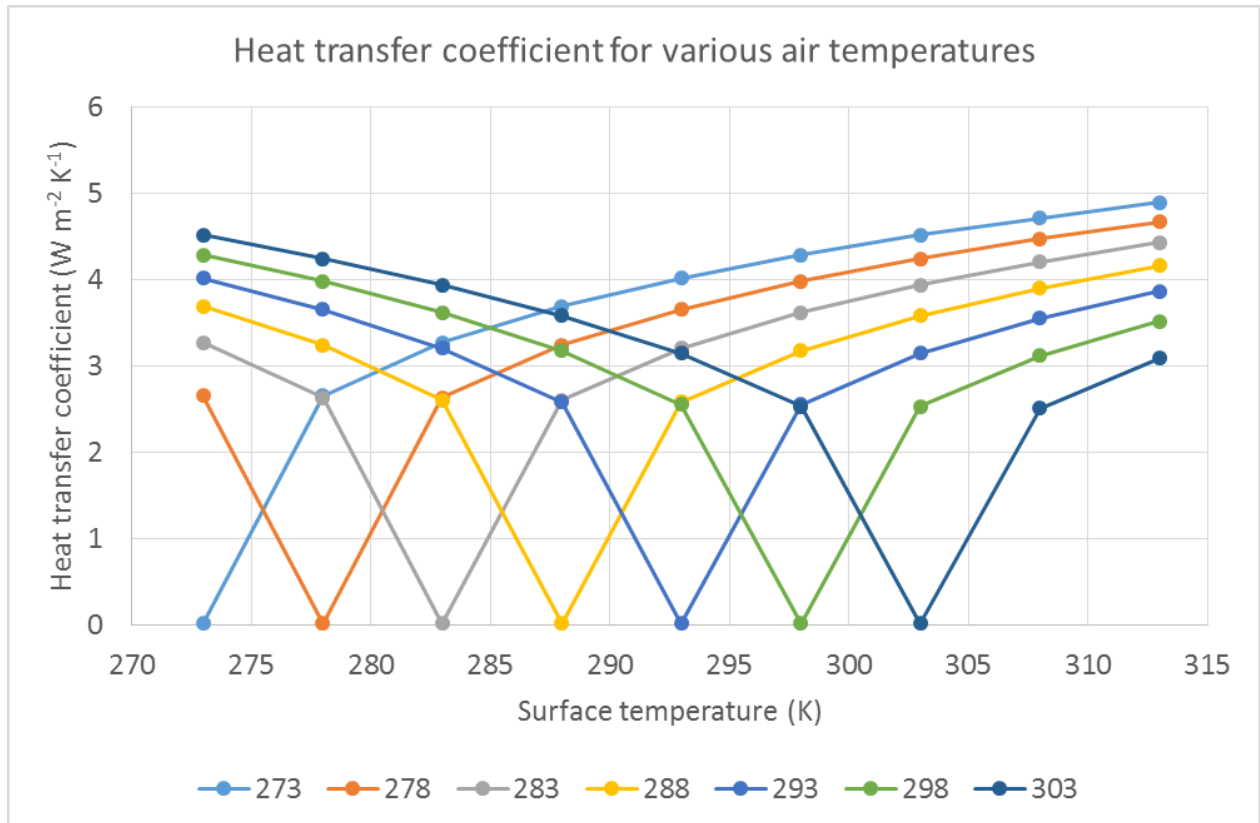
Figure 3: Heat transfer coefficient as a function of surface temperature for different air temperatures.

The main point to note from this graph is that the curves are essentially a single curve shifted to the left or right, meaning that the coefficient is well approximated by a function of temperature difference. Replotting all the results against temperature difference emphasises this, as is shown in figure 4. The variation in coefficient values for each temperature difference is small.

More detailed calculations were therefore carried out at a fixed air temperature (293 K, chosen as being typical for the UK). This choice of temperature is completely arbitrary because figure 4 shows that the coefficient is a function of temperature difference rather than temperature. The heat transfer coefficient was calculated every 0.5 K of temperature difference between -20 K and + 20 K, and the resulting heat flux was calculated from equation (12). The results are shown in figure 5, along with a straight line fit to the results. The straight line fits the values well, although it underestimates heat losses at large temperature differences and overestimates losses for small temperature differences. The gradient of the straight line fit is the best estimate of a constant heat transfer coefficient. Given the goodness of fit (relative error is less than 10% throughout), the heat transfer coefficient was fixed at a value of 3.6 W m^{-2} K^{-1} throughout the subsequent model runs.
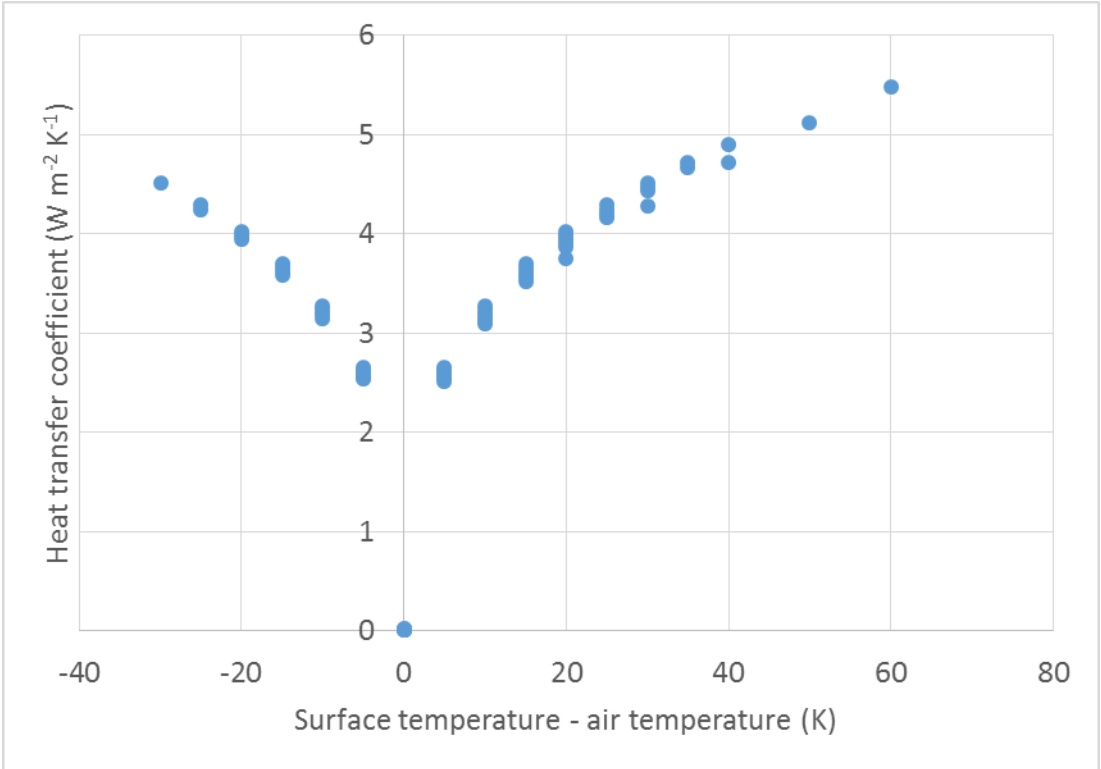
Figure 4: Heat transfer coefficient as a function of surface temperature minus air temperature.
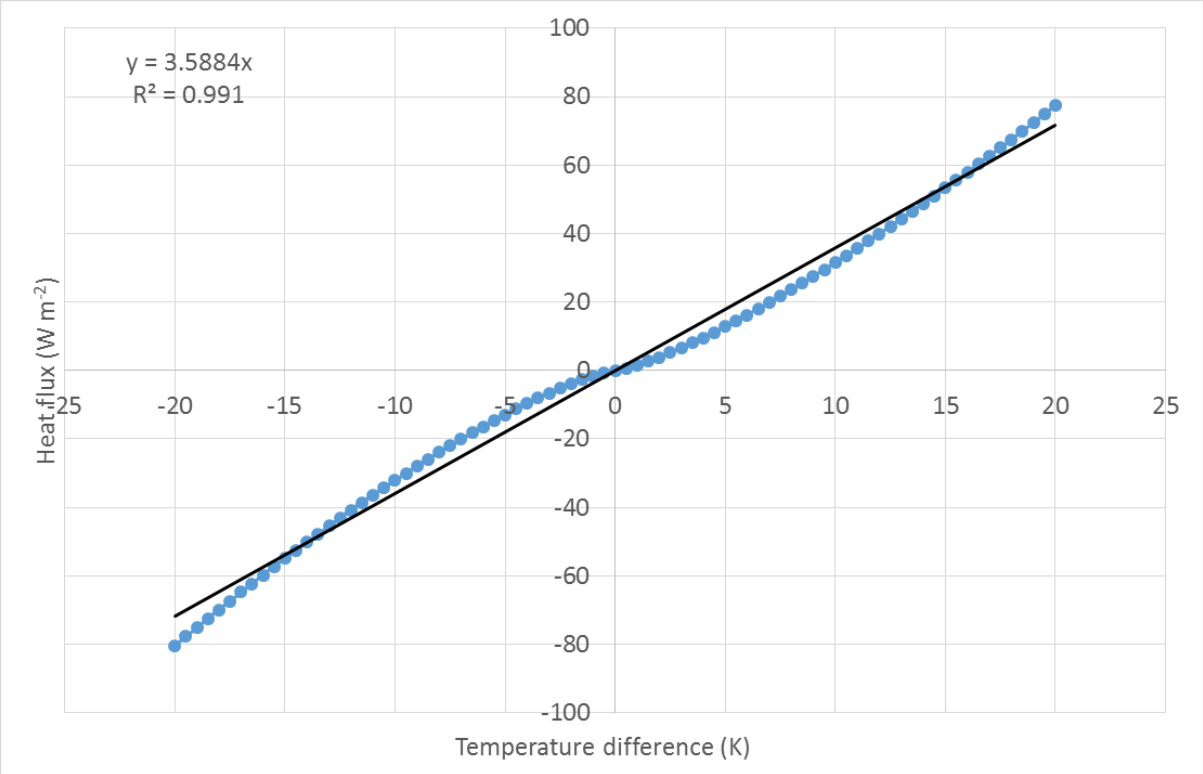

Figure 5: Heat flux as a function of surface temperature minus air temperature and straight line fit.

4   DISCUSSION AND ASSESSMENT OF ASSUMPTIONS

This section discusses some of the assumptions that have been made in the model development above, and assesses their impact on the model results. In some cases additional models of buildings have been run, and the results will be presented as changes in temperature without discussing the temperatures in detail as a detailed discussion of the results of each model will be given in section 5.

4.1 QUASI-STATIC MODEL AND NEGLIGIBLE THERMAL MASS

In order to check the validity of the assumption that the thermal mass of the wall is negligible, a simple one-dimensional model was constructed of the transient heat flow through a wall using a finite difference approach to solve the equation

$$\rho c_p \frac{\partial T}{\partial t} = -\frac{\partial^2 T}{\partial x^2} \tag{25}$$

The inside air temperature and outside air temperature were taken from the Portland Grove measurement data set, as these had a high internal air temperature and a low external air temperature and so would provide the most challenging conditions. The surface temperature of the wall was calculated using the transient one-dimensional model and the quasi-static approach given in equations (18) to (24) above, starting from the same initial conditions of equilibrium. The internal and external surface temperatures given by the two models are compared in figure 6 below. The difference between the results of the two models was less than 1 K throughout, meaning that the quasi-static model is a good approximation and is suitable for this data set.
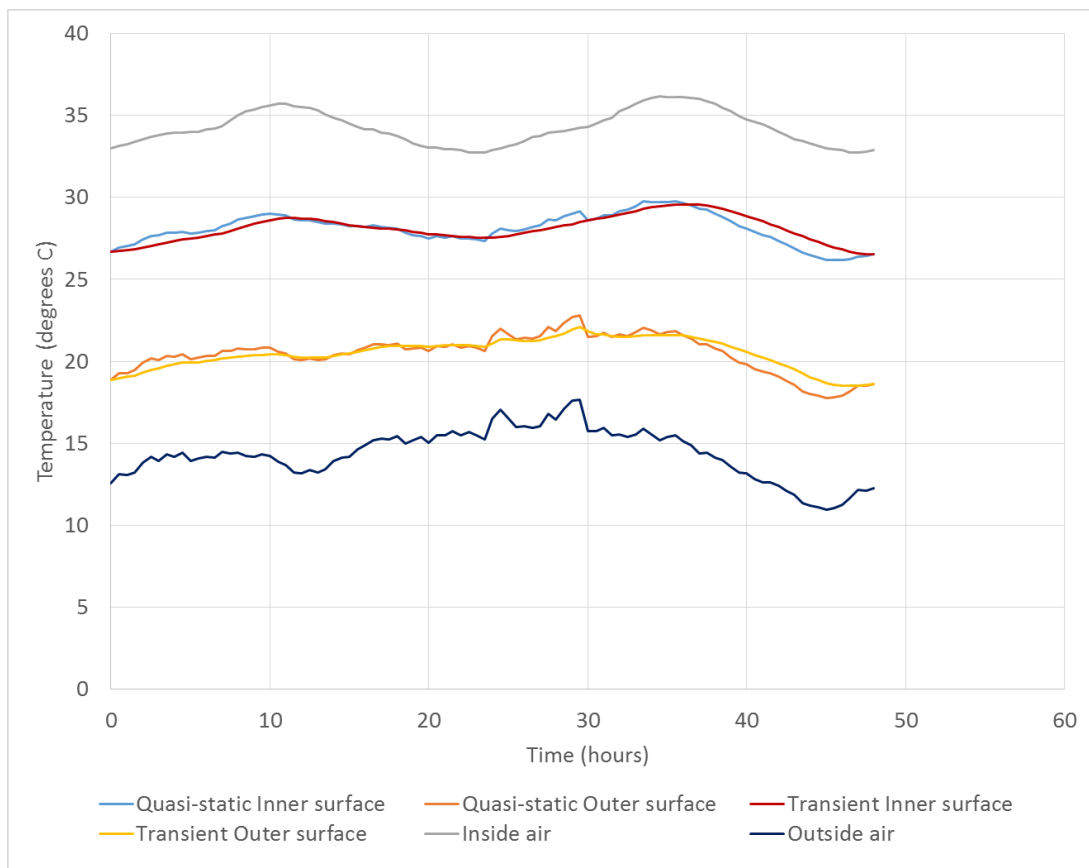
Figure 6: Comparison of a transient and quasi-static model for heat flow through a brick wall.

These models entirely neglect the effects of solar heating. Since the data were gathered in Greater Manchester in the winter, it is likely that the effects of the sun can be neglected. In order to test the effects of sunshine, another 1-D model was built that included incoming solar radiation (set at

15

600 W m^{-2}, an upper bound for the north-west of England according to CIBSE data [21]) and radiative losses to air temperature from the heated wall. The sun was assumed to be shining for eight hours of the day. Results of the transient model with solar radiation and the equivalent quasi-static model are shown in figure 7. The approach proposed for calculating the inner temperature of a wall of known outer temperature as described in equations (23) and (24) in section 3.4.1 is also shown (labelled "inner given outer"). The chart shows the variations of the calculated internal and external wall temperatures over a two day period.
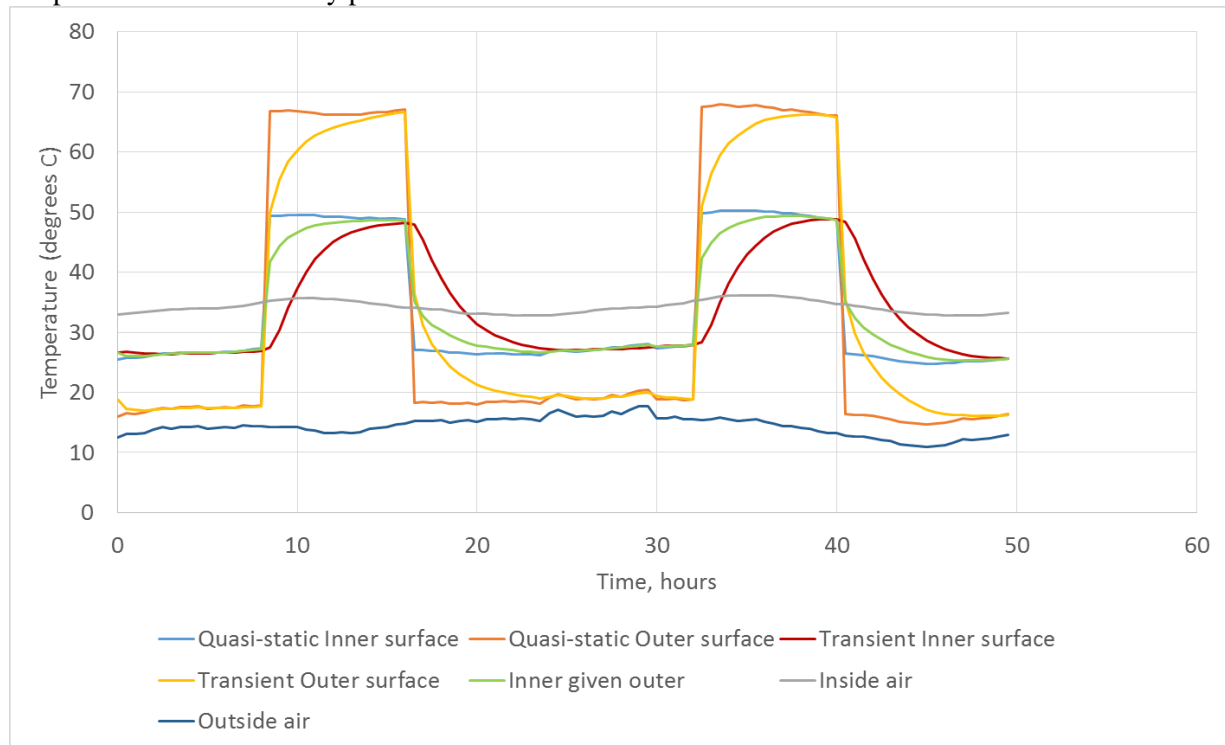
Figure 7: Comparison of transient and quasi-static models for heat flow through a brick wall when radiative solar heating is significant.

It is clear that the quasi-static model over-predicts the temperature when sunshine is heating the building, and under-predicts the temperature of the building as it cools, as would be expected from the neglect of thermal mass.

As was noted earlier in this report, it is likely that the solar heating during the period over which the validation data were gathered is insignificant so this lack does not compromise the validation of the models in this report, but solar heating will be considered during the next stage of the project, and it is clear that a transient model will need to be used for that work.

4.2 TRANSFORMER FIN APPROXIMATION

The test model for the transformer fin consisted of a 1 m cube containing a solid box representing the transformer, and a set of fins. The fins were modelled in two ways, either as a set of ten parallel plates of finite thickness (see figure 8a) or as a volume of the same size as the fins with equivalent heat transfer characteristics (figure 8b). The heat gains from the solid box and the losses through the walls, ceiling and floor were taken to be convective. The fins were taken to be at a uniform temperature of 313 K. An inlet and an outlet were included in the model. The incoming air was taken to have a temperature of 293 K and to be at zero pressure relative to background air pressure for that height. The outlet was set at zero relative pressure and backflow was suppressed. The power (i.e. rate of change of energy) of the air leaving through the outlet (kinetic and thermal) was calculated from a surface integral (rate of energy transfer is relevant because the model is a static snapshot). The effects of the separation of the transformer fins from the wall was tested by running a series of models at different separations. The power entering the box through the inlet was also calculated.

Results of the models are summarised in table 2. The power added to the air is shown (i.e. power leaving – power in) as this is the most important feature of the fin approximation. The difference between the two models is less than 5%. There appears to be little variation of the error with the separation from the wall.

Table 2: Results of test model for fin approximation.

Separation from wall (m)	Power added with volume fins (W)	Power added with detailed fins (W)	Difference (detailed – volume) relative to detailed fin model
0.25	85.2	83.3	-0.022
0.2	85.0	86.3	0.015
0.15	86.3	85.8	-0.006
0.1	89.6	87.9	-0.019
0.05	87.9	89.3	0.016
0.01	84.6	88.8	0.047
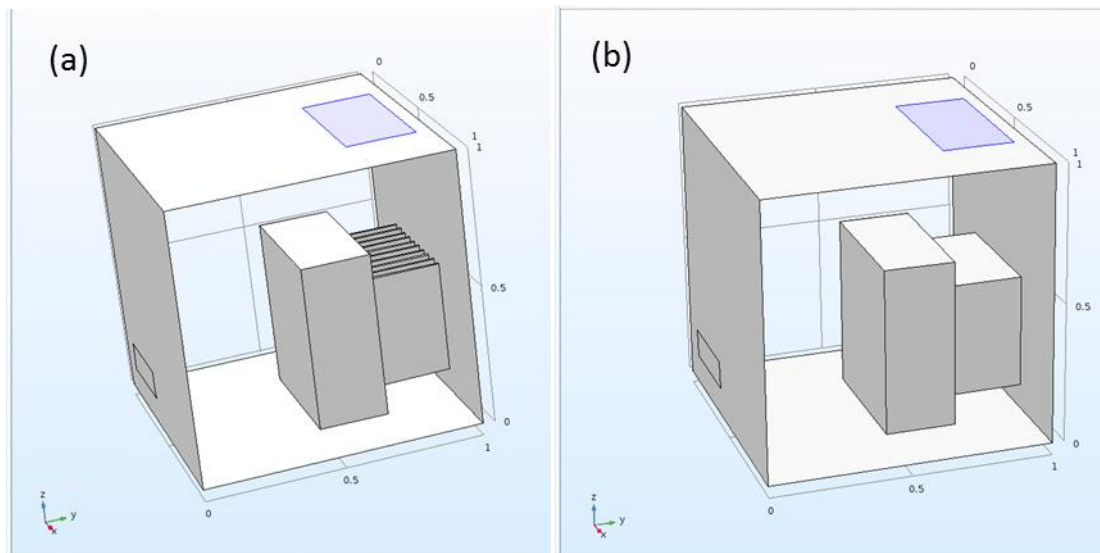
Figure 8: Test models for the fin approximation with detailed fins (a) and a volumetric heat source (b). Front and back walls have been removed for clarity but are present in the model.

Figure 9 shows a direct comparison between two typical models with a wall separation of 0.01 m. The left hand plot shows the model with detailed fins, and the right hand plot shows the model with the volume approximation of the fins. The colour contours show the temperature distribution, and the arrows show the air flow (the larger the arrow the higher the velocity). The two plots are in good agreement. There is a temperature difference of about 2 K in the peak local air temperature, with the volumetric heat source under-predicting the temperature. This is an additional potential source of error in the model.
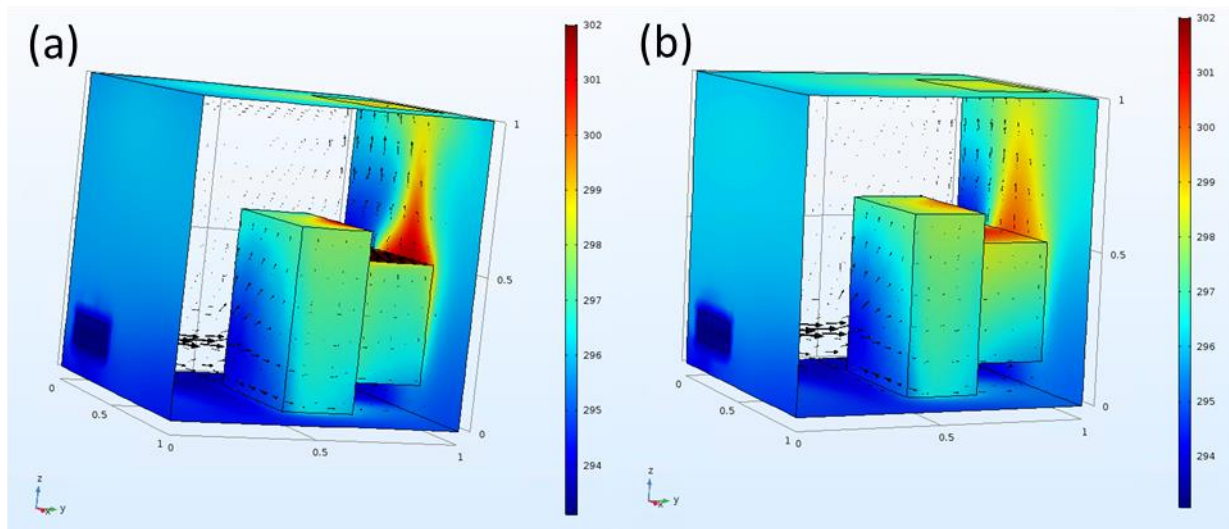
Figure 9: Typical results of the test models with detailed fins (a) and a volumetric heat source (b). Contour colours represent temperature, arrows represent air velocity.

4.3 WEATHER CONDITIONS

It was noted in section 4.1 that for the likely level of sunshine in north-west England in the winter, solar heating can be neglected. Solar heating will be key to assessment of the cooling technologies during phase 2 of this project, and will be built into transient models at that point.

Rain could potentially cool a building as it collects or evaporates. Calculation of the effects of this process on the building temperature is challenging, because it depends on the air temperature, humidity, and velocity and on the building temperature. Given that overheating of the substation building is a key concern of this work, rain is an additional source of the desired cooling and so need not be taken into account when considering cooling performance. The effect of any rain evaporation on the validation data is likely to be small because evaporation at low air temperatures occurs over a long enough time scale that any effects on wall temperature will be small.

Wind can alter the pressure distribution around a building, which would affect the flow through the inlets of a building. A model has been run with a positive pressure of 25 Pa at one inlet to simulate a wind impinging on that wall. The pressure was calculated by taking a typical mean wind speed in the UK of 5 ms^{-1} from data from [25] (note that this is wind speed at 25 m above ground and so will be an over-estimate) and using the wind pressure table at [26] to estimate the ensuing pressure.

As would be expected, the increase in pressure on one side of the building led to an increased air velocity at the inlet on that side of the building. Figure 10 shows results for models with and without wind as a colour contour plot for the air temperature and arrows whose lengths are proportional to air velocity. The air flow with wind is dominated by the inward jet from the vent, reducing the average air temperature inside the building. Calculation of the power being lost from the transformer fins for each model shows that the model with wind loses about 9 % more energy per second than the model without wind (2249 W vs. 2065 W). The result suggests that wind ingress improves cooling as it injects cold air into the building and disrupts circulation, provided the incoming wind is able to leave the building through a vent that is on a wall that is not under wind pressure.

The results of the wind model suggest that the vents should not all be placed on one side of the building to avoid an incoming wind stopping air leaving the building and to benefit from any wind that does occur.
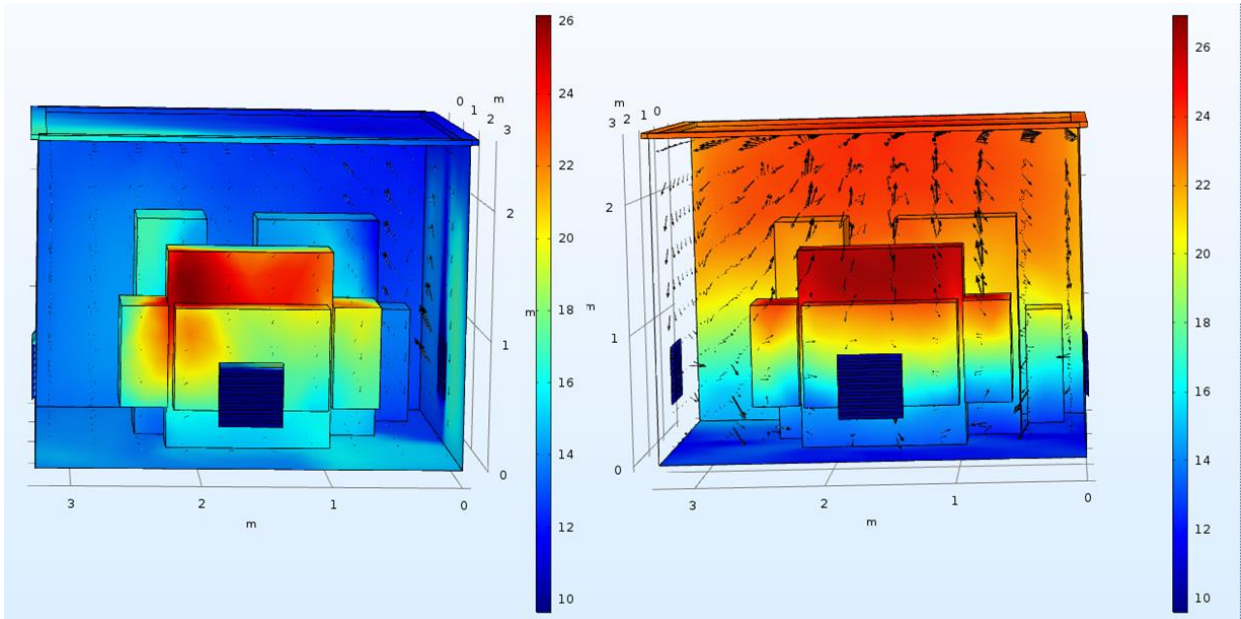
Figure 10: Air flow and temperature contours with (left) and without (right) the effects of wind.

4.4 CLEARNESS OF VENTS

In many cases the vents of substations are not clear. The louvres and meshes used to prevent ingress of rain and fauna also collect leaves and other airborne detritus, leading to partial blocking of vents over time. As a result, it is possible that some of the vents modelled are not fully clear.

A worst case scenario has been tested by completely blocking one vent of a model. A model was run blocking a vent known to give inflow under normal conditions. Figure 11 shows a direct comparison between the model with the blocked vent (left plot) and the open vent (right plot).
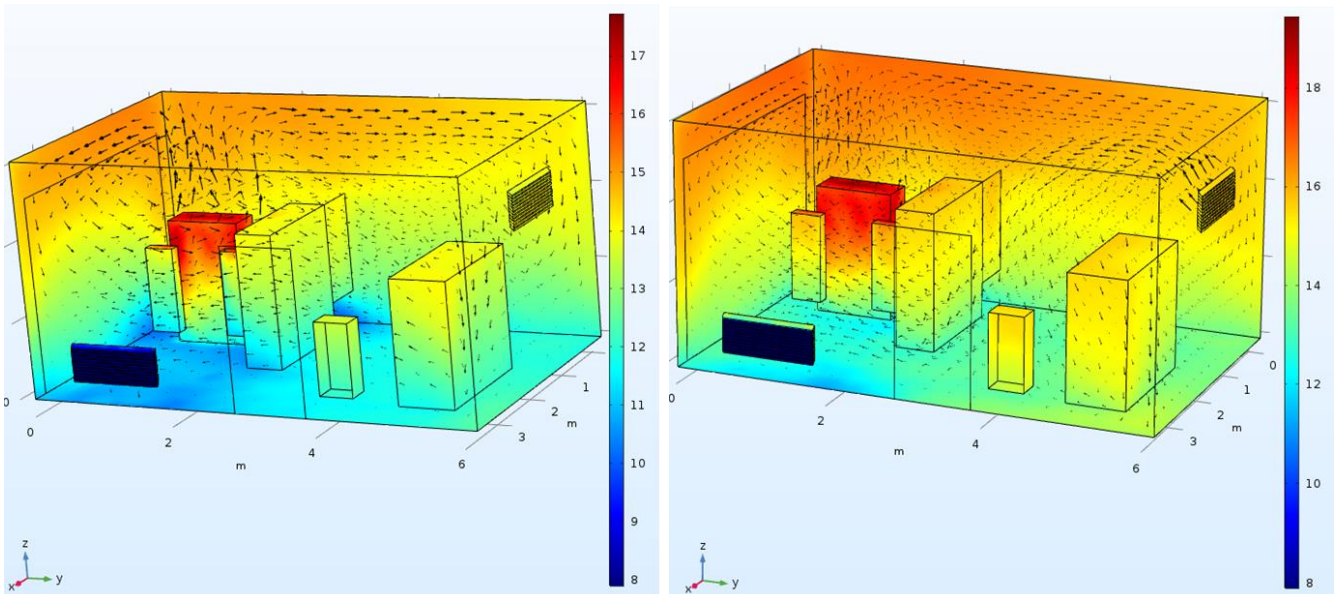
Figure 11: Air flow and temperature contours with (left) and without (right) a blocked vent. An additional vent is situated behind the transformer. (see figure 30).

The difference between the two figures is comparatively small, suggesting that the flow is dominated by recirculation and that the vent is not a very large source of cold air. The version with the blocked vent shows a lower maximum air temperature, because the unblocked vents are closer to the

19

transformer and so the cold air they supply impinges on the transformer more quickly. The same effects leads to the model with the blocked vent predicting a higher cooling power than the unblocked vent (521 W vs. 465 W).

4.5 SIGNIFICANCE OF OTHER HEAT SOURCES

Whilst the transformer is the most significant heat source due to its large surface area and high temperature, other sources of heat exist within the substations. The amount of heat energy transferred to the air from a hot object depends on the temperature distribution of the object, the temperature of the air, the surface area of the object, and the convection coefficient associated with the object geometry.

It is known that Joule heating of the cables occurs, proportional to the square of the current, and other components of the switchgear are also affected. It was expected that the comparatively small surface area of cables and the localisation of the heating within switch gear meant it would be insignificant in comparison with the transformer, but this assumption is explored below. It is very difficult to assign a suitable temperature distribution to objects like the switchgear, because it is not clear how far the heat spreads when it heats up (Figure 12 shows a thermal image[4] of a typical heated switchgear showing the complexity). It is therefore useful to see what the effect of including extra heat sources in the model is.

Figure 12: Thermal image of LV switchgear taken in Wentworth Road.

---

4 Thermal images are famously problematic when diagnosing temperature distributions, since the indicated temperature is a function of both temperature and surface emissivity (which describes how well an object emits infrared energy, or heat), so that for example a shiny object and a dull object, both at the same temperature, will appear to be at significantly different temperatures (the dull object will appear hotter, as will holes and crevices). They should therefore be interpreted with great care.

Two models were used to look at the effects of extra heat sources. Both models included a cuboid representing the switchgear, and both buildings had measurements of the temperature of low voltage cables in more than one place.

The Town Bridge site encases the switchgear in a cabinet, and the temperature of the inside of the cabinet is measured at a high and a low position. These two measurements were used to assign a distribution to the entire surface of the cabinet. This approximation is reasonable because the switchgear is enclosed. The maximum difference in calculated air temperatures observed was less than 0.3 °C. The comparison between measured values and the results of the two models is shown in figure 13.
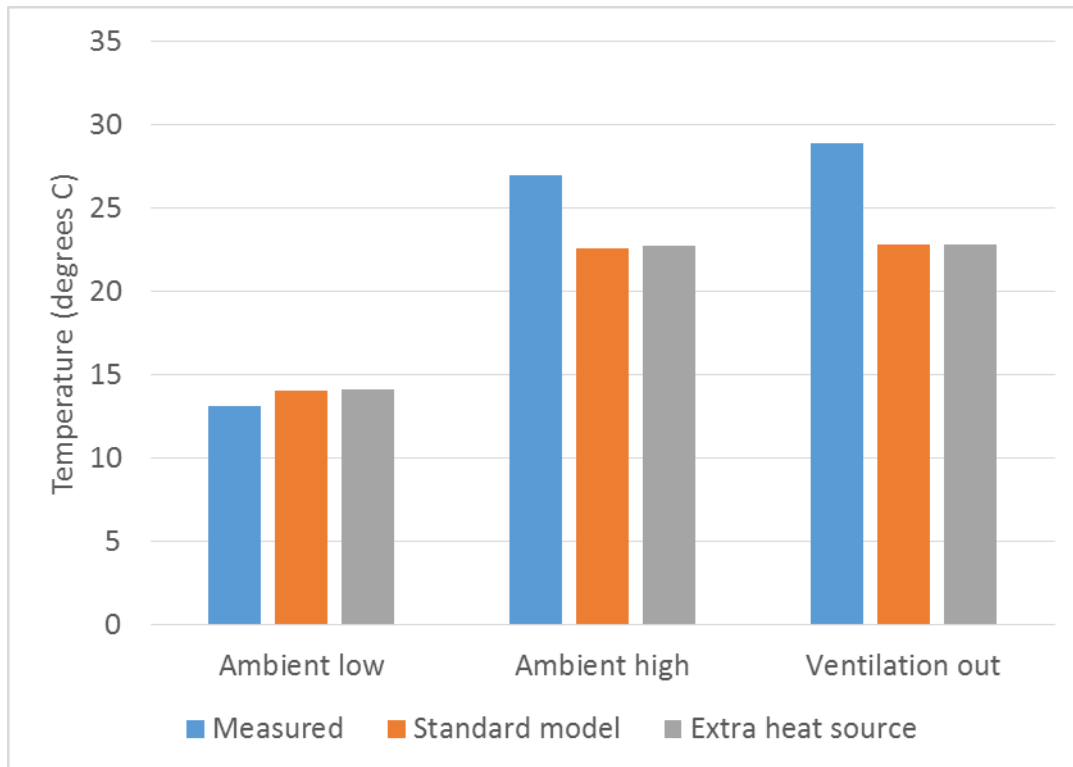
Figure 13: Comparison of measured values with model results with and without additional heat sources for Town Bridge.

The Wentworth Road site has an open switchgear, as shown in figure 12, and the cuboid representing the structure in the model is larger than its true surface area but in the absence of any reliable information about the temperature distribution on the surface, a temperature distribution dependent on the height above ground level was defined over the entire cuboid. This approach is likely to lead to an over-estimate of the amount of energy going into the air, and hence an over-estimate of air temperature. The heat distribution shown in figure 12 suggests that the air temperature low down is most likely to be over-estimated. Figure 14 shows a comparison between the measured value and the results of the original model and the model with the extra heat source. The figure shows the expected increase in temperature, with the typical difference between the two models being about 2.5 °C. The model with the extra heat source over-predicts the temperature low down (Ambient low), as anticipated, but is more accurate for the air temperatures high up (Ventilation out and Ambient high).

The results of these two models suggest that in some cases the extra heat sources are significant and in others they are not. In theory the models could be adjusted until better agreement for all measured temperatures was achieved, but this would be a model of one specific situation and would not necessarily apply if the cable heating pattern changed, as would be expected when the configuration of current changed. Tweaking models to fit results without physical justification can lead to poor predictive qualities and less understanding of the system. As a result, the decision has been taken to

neglect the heat sources that are not the transformer, but to acknowledge that they are a potentially significant source of error, particularly for the measurements made high up within the substation building. Whilst it is likely that as demand increases and transformers become more heavily loaded the switchgear etc. will become a more significant source of heat, it is also likely that the approaches used to cool the transformer will also either cool other heat sources as well, or can be adapted/extended to do so. Any technique that enables the removal of hot air from the substation building will cool all heat sources effectively.
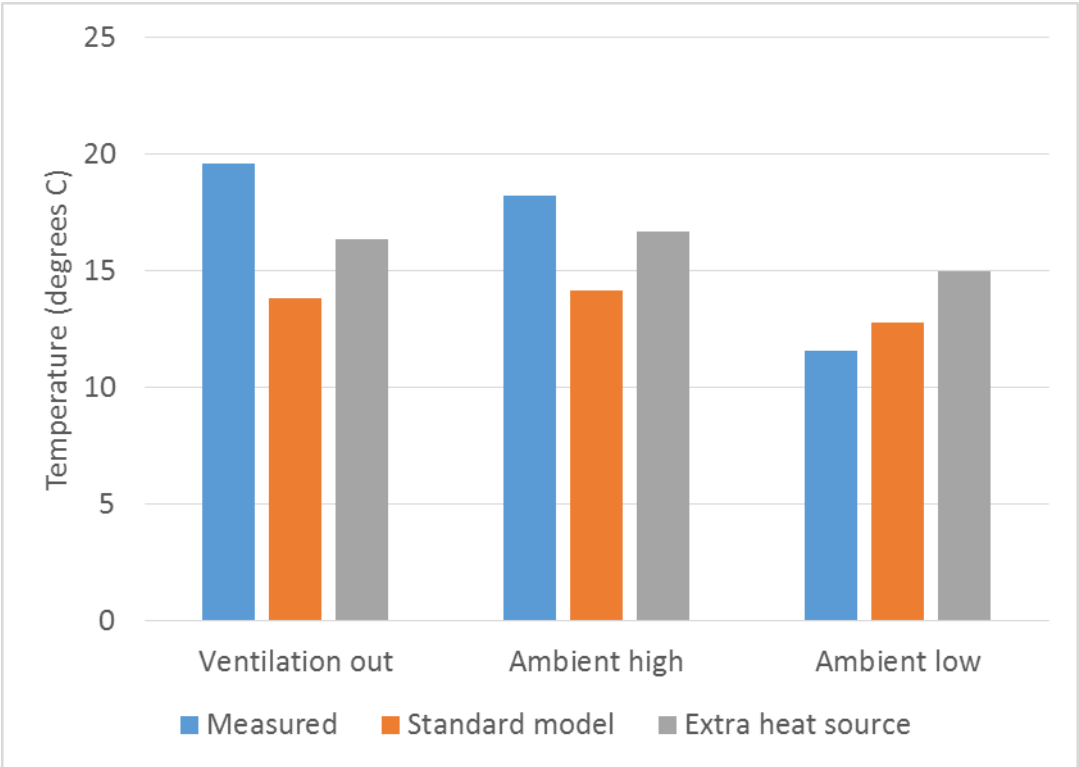
Figure 14: Comparison of measured values with model results with and without additional heat sources for Wentworth Road.

5   RESULTS

Six full-scale models of buildings have been constructed. The top oil, bottom oil, and air inlet temperatures used in each model are listed in table 3, along with the time and date at which the values were measured. Top oil and bottom oil are both measurements of the temperature of the transformer and are used to define the temperature distribution of the fins and the surface of the transformer within the model. The air inlet temperature is used to define the temperature of the air entering the building in the model.

Table 3: Temperatures used as boundary conditions in the models and time at which those temperatures were measured.

Site	Time & date of measurement	Top oil temperature (°C)	Bottom oil temperature (°C)	Ventilation in temperature (°C)
Acorn Street	08/01/2017, 20:30	48.5	27.125	9.4375
Emmanuel Street	19/12/2016, 21:00	31.3125	21.75	8
Portland Grove	28/01/2017, 19:30	56.75	45.0625	7.8125
Southgate Industrial Estate	24/01/2017, 17:00	22.3125	13.8125	8.0625
Town Bridge	07/02/2017, 16:00	47.6875	30.25	9.6875
Wentworth Road	02/03/2017, 20:30	42.8125	23.75	7.9375

5.1 RESULTS OF THE INITIAL MODEL DEVELOPMENT

The initial versions of the model followed the recommendations in the literature and used turbulent flow to model the air movement, despite the fact that the flow is driven by temperature differences rather than by fans etc., so the air velocity is lower than that typically required for turbulent flow.

These initial versions of the model did not agree well with measurement. In general the models predicted a lower level of thermal stratification than was seen in the measurements. Various attempts were made to adjust the model to improve the validation. These attempts included changing the boundary condition at the floor, increasing the amount of energy put into the room to try and account for possible other heat sources, allowing more air flow through the vents, switching to a transient turbulent model, and using a laminar flow model.

Detailed results of these various models are not presented here, but overall the only alteration of the model that led to increased thermal stratification and an improved agreement with measured values was the use of a laminar flow model, despite the results of the literature review. It is not that surprising that laminar flow gives better results, because the air velocities in flows driven purely by comparatively small thermal gradients are often sufficiently low that flows are generally in the laminar regime. It is intended to report this result in an appropriate scientific journal.

5.2 VALIDATION AND DISCUSSION OF SITE MODELS

Note throughout that the temperature distributions shown are air temperature distributions and not surface temperature distributions, so for instance the temperature of the transformer shown in the figures will always be lower than the oil temperatures shown in table 3 because the air passing through the transformer fins does not reach the temperature of the fins themselves.

5.2.1   Acorn Street

A diagram of the contents of the Acorn Street building is shown in figure 15. The building includes wall-mounted LV board and a large HV switchgear unit as well as the transformer. The transformer is in a room partially separated from the rest of the kit by a brick wall. Ventilation is via air bricks.
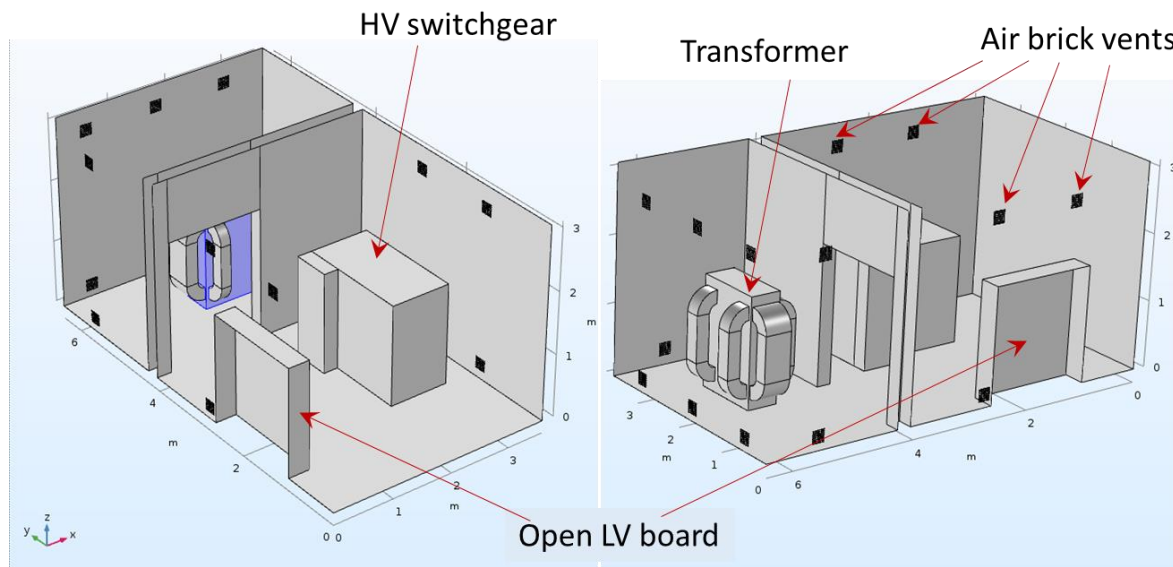

Figure 15: Acorn Street substation shown from two angles.

Figure 16 shows the air temperature distribution and air flow within the model of Acorn Street. The temperature difference between the air passing through the transformer fins and the air temperature by the walls is approximately 4 °C, suggesting that the hot air is not leaving the building but is heating the walls instead. Close examination of the air velocity at the vent bricks shows that there is very little airflow passing through them. The air recirculated and the room is only cooled by losses through the walls, floor and ceiling.

Figure 17 shows a direct comparison between the measured air temperatures at various positions and the model results. The agreement is generally very good, with the differences between measured and modelled values being less than 1 °C in two out of three locations. The ambient temperature measured high up in the building is under-predicted by the model, with the difference being about 2.2 °C. The surface temperature of the LV cable connected to the transformer has been measured and is at a temperature midway between the top and bottom oil temperatures, confirming that the cables are also a source of heat that is raising the air temperature high up in the building.
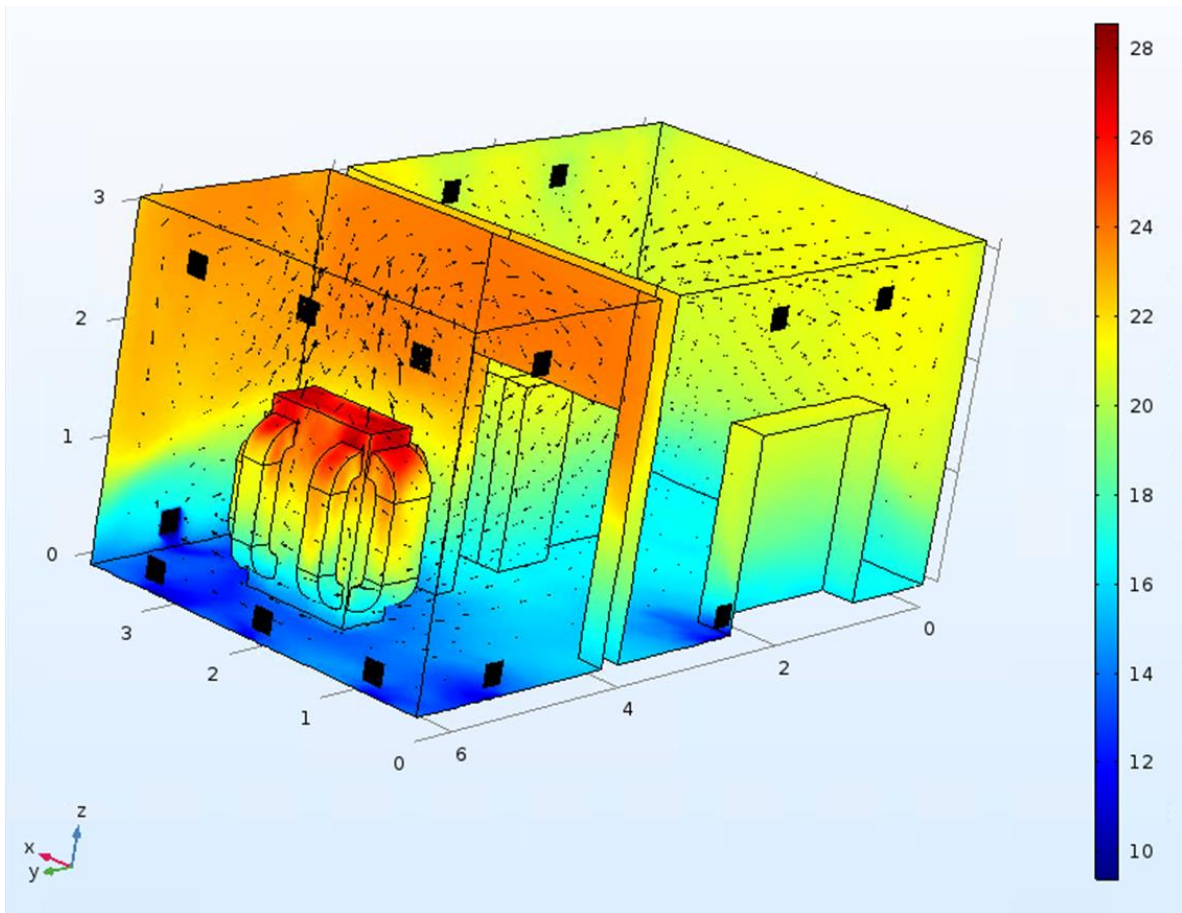
Figure 16: Air flow and temperature distribution within Acorn Street.
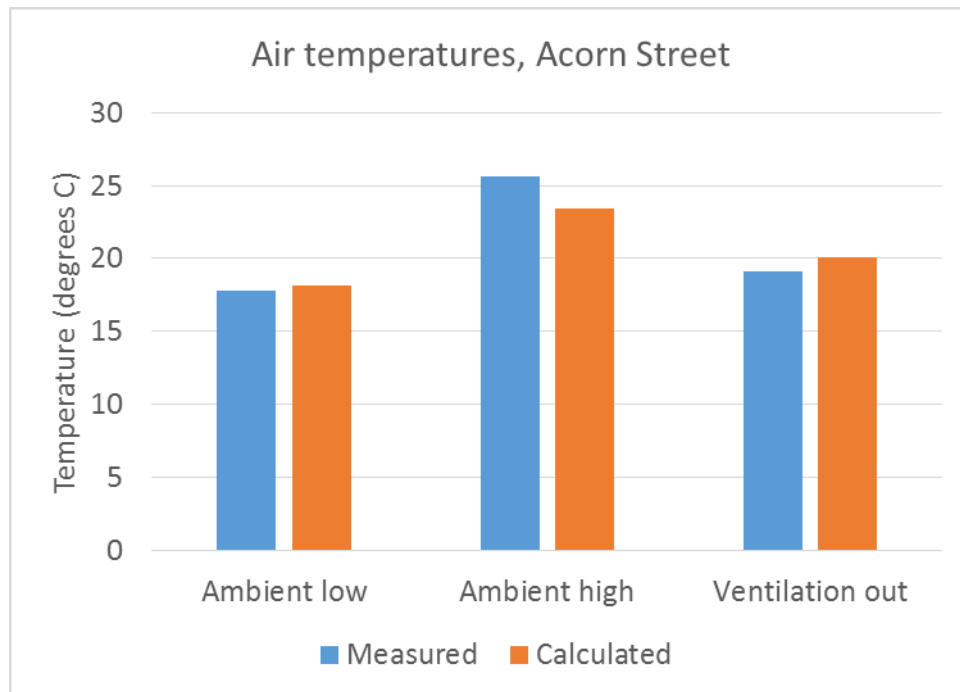
Figure 17: Comparison between measurement and model results for Acorn Street.

5.2.2   Emmanuel Street

Figure 18 shows the contents of the Emmanuel Street building. The LV board, remote terminal unit (RTU), and ring main unit (RMU) are all comparatively small and are well separated from the transformer. Ventilation is through two door vents and four vents in elevated "chimneys" in the roof.
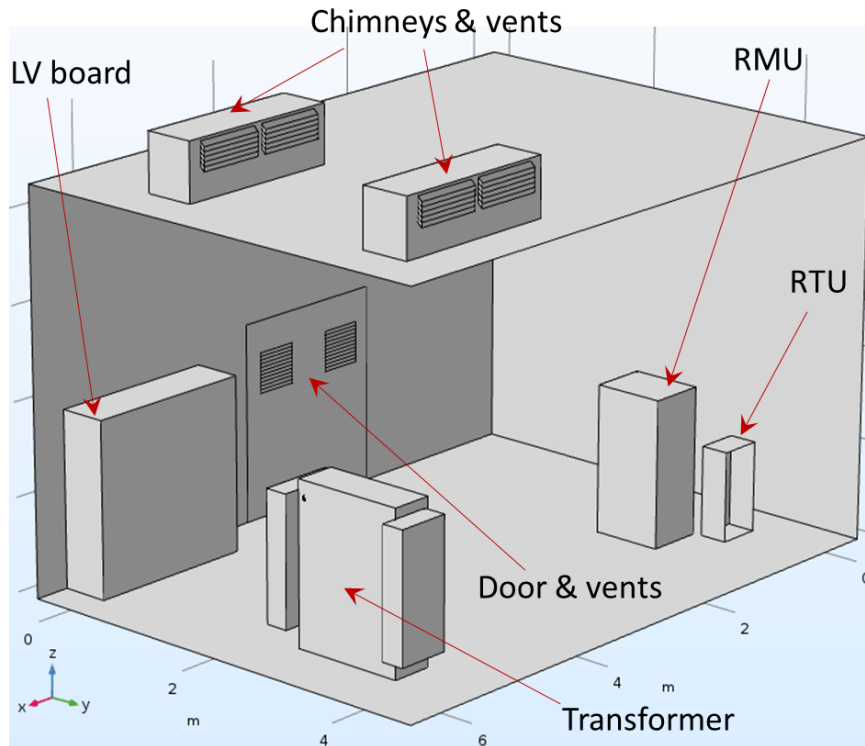

Figure 18: Internal layout of Emmanuel Street.

Figure 19 shows the temperature distribution and air flow within the building. The transformer is not under heavy load (as listed in table 3, the top oil temperature is only 31 °C) so the maximum air temperature of just under 20 °C is not a lot hotter than the ambient temperature and the walls do not get heated significantly.

Detailed examination of the air flow at the vents shows that very little air is coming in through the door vents. The majority of the air coming in enters through the sets of roof vents furthest from the transformer. The roof vents nearer to the transformer allow some of the hot air to leave the building, which is why the air in the chimney nearer to the transformer is hotter than the one further from the transformer.

Figure 20 shows a direct comparison between measured and calculated air temperature values. Agreement is very good, with the maximum difference being about 1 °C. There is not ventilation out measurement for this building as the roof vents are somewhat inaccessible.
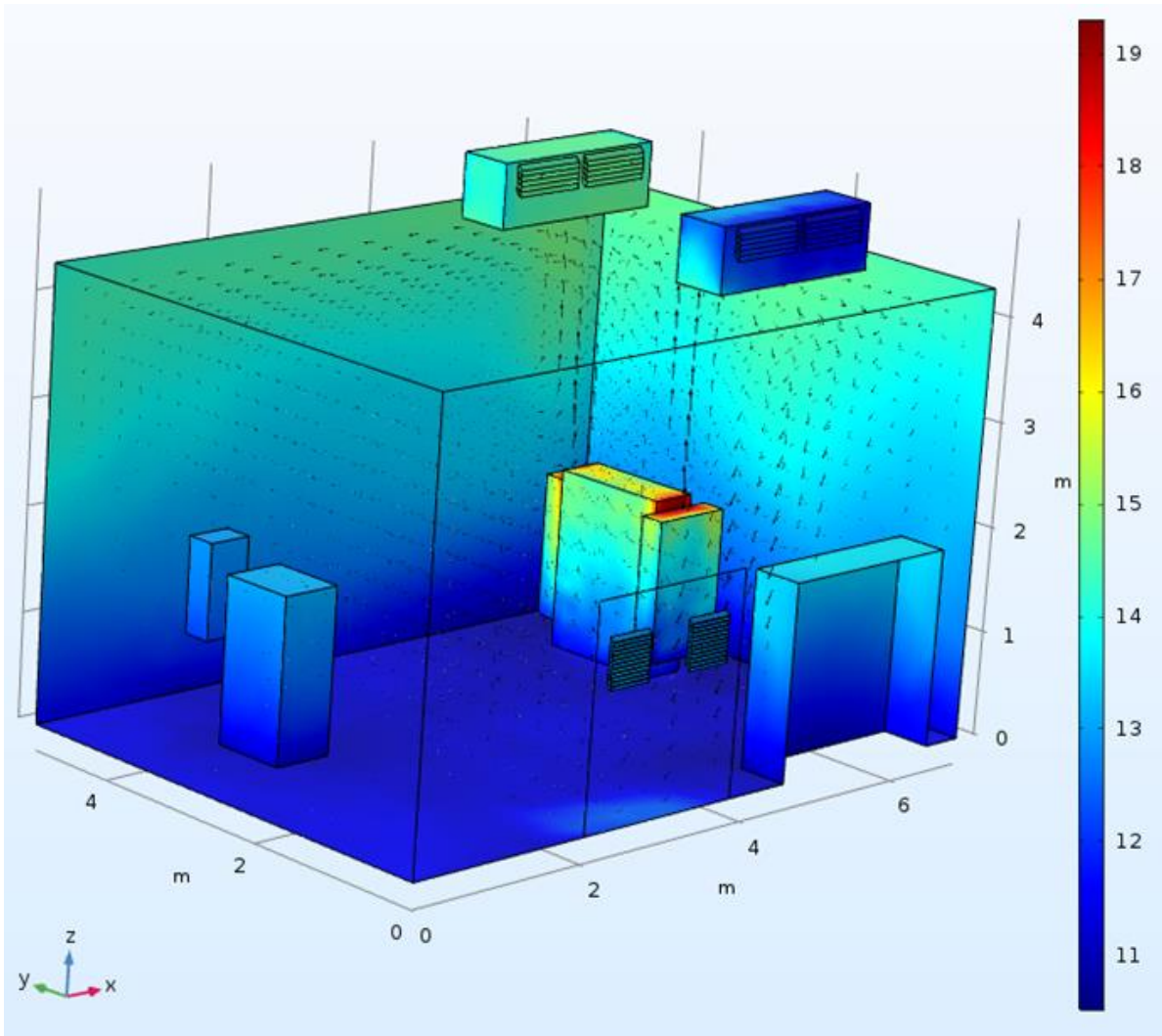
Figure 19: Air flow and temperature distribution within Emmanuel Street.
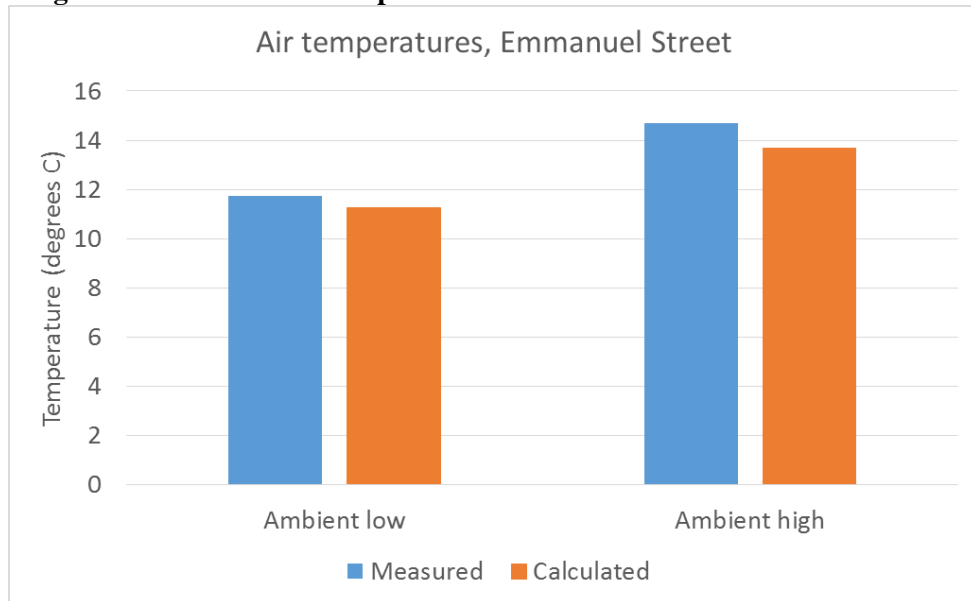

Figure 20: Comparison between measurement and model results for Emmanuel Street.

5.2.3   Portland Grove

Figure 21 shows the position of the various pieces of equipment within the Portland Grove building. The building includes an LV board and HV switchgear. The LV board is separated from the main body of the building by a wooden wall, but the wall does not reach the ceiling. Ventilation is through door vents and air bricks.
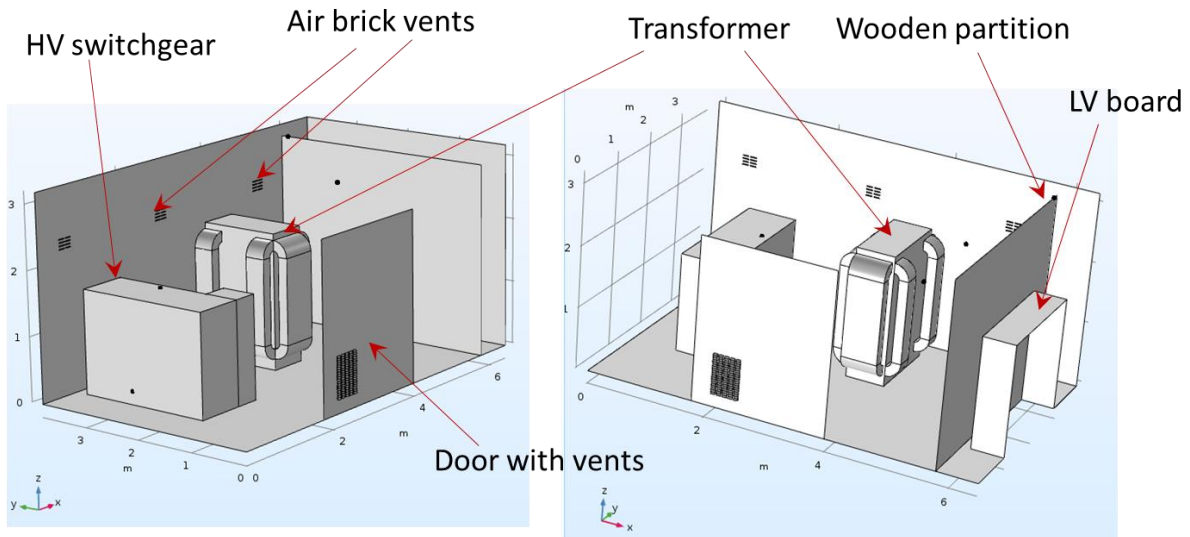

Figure 21: Internal layout of Portland Grove substation from two angles.

Figure 22 shows the air temperature distribution and air flow in the Portland Grove building. The temperature of the air by the walls is much higher than the ambient air temperature throughout the building, and the air flow direction arrows show that the air is recirculating and heating the building rather than leaving through the vents. A close examination of the air velocity at the vents confirms that very little flow in or out of the building occurs.
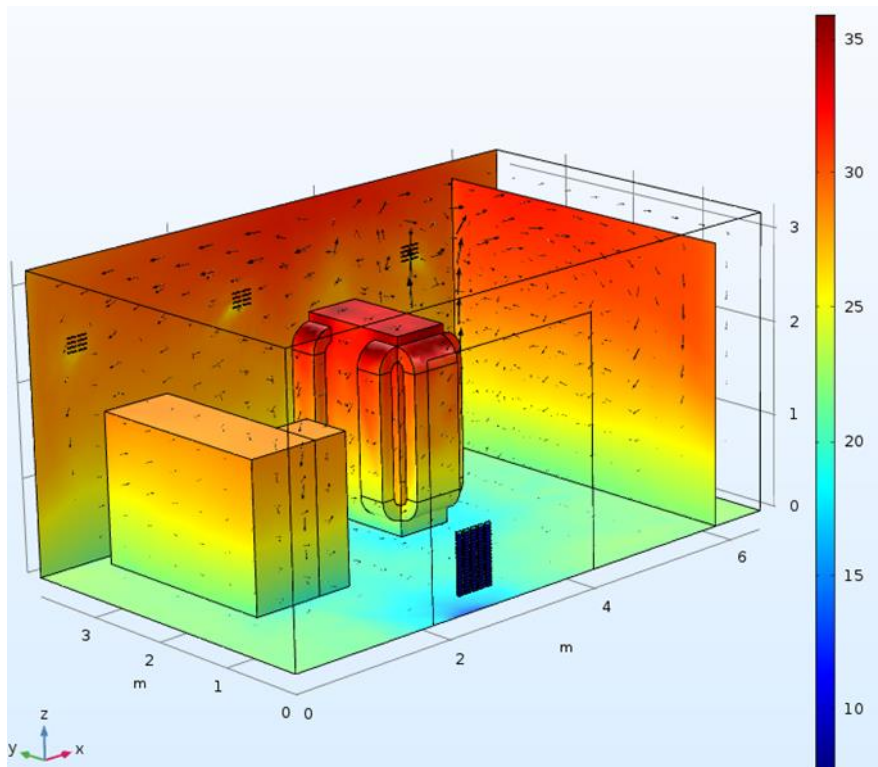
Figure 22: Air flow and temperature distribution within Portland Grove.
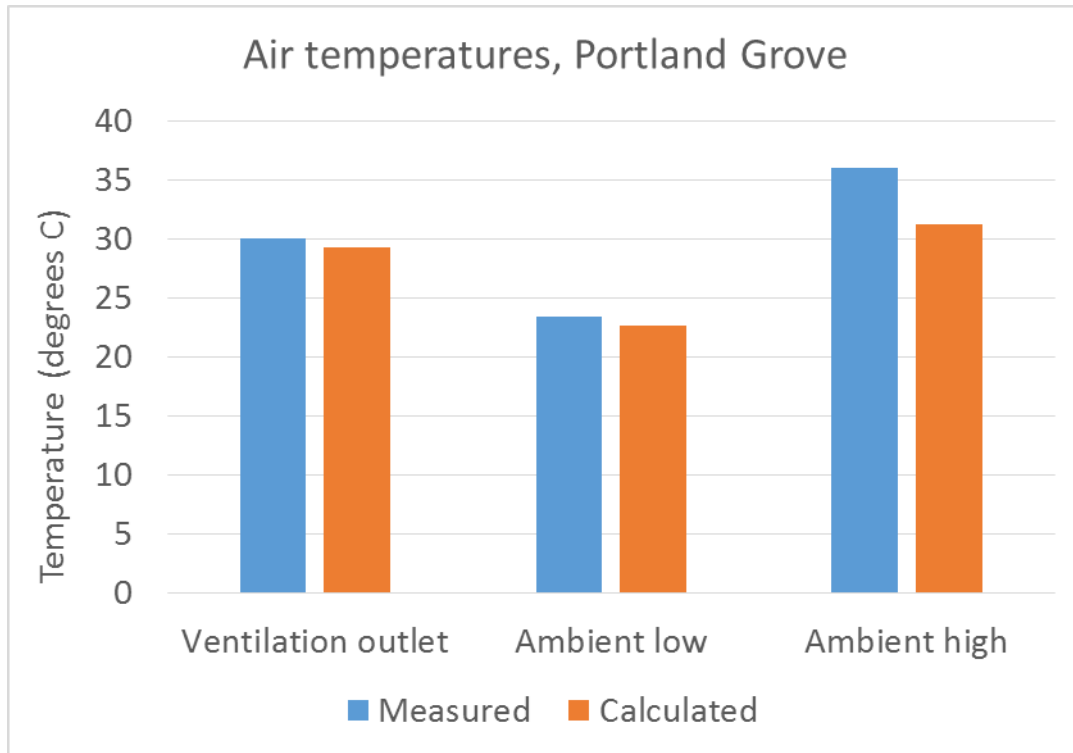
Figure 23: Comparison between measurement and model results for Portland Grove.

Figure 23 shows a direct comparison of the measured ambient temperatures and the model results. The agreement is generally good, with the ventilation outlet and ambient low model results differing from the measurement by less than 1 °C. The ambient high results differ by about 4.8 °C, with the model under-predicting the temperature. Examination of the other temperature measurements made in the building show that the LV cables reach a temperature of about 45 °C. The LV temperature sensor was placed behind the wooden partition, and the air high temperature sensor was placed at the top of the wooden partition, so it is likely that the air high temperature will be strongly affected by the heat emitted by the LV cables and that the omission of this source of heat has led to the discrepancy.

5.2.4   Southgate Industrial Estate

Figure 24 shows the internal layout of Southgate Industrial Estate. The building is a GFRP structure containing a transformer, an LV unit and an RMU. The LV unit is inside a cabinet, and the three objects are close together. The roof structure includes a baffled vent as sketched in figure 1, and the walls have vents with an angled section at 45° to the vertical. The door is on the face shown with no vents (facing towards the viewer on the left-hand half of figure 24).

Figure 25 shows the temperature distribution and air flow within the model of Southgate Industrial Estate. The hot-spots on some of the walls suggest that the hot air does not leave at the roof vent, but recirculates and heats the walls. Closer examination of the air flow at the vents shows that some air enters through the roof vent and that air leaves through the vents in the walls. The air flows up through the transformer fins, is cooled at the roof, and flows downwards next to the wall, effectively entraining air from the roof vent. The downwards flow at the wall is then steered through the vent by the angled section. As this is a GFRP building, the heating of the air next to the walls is beneficial since heat leaves through the walls easily due to the high U-value (see section 3.4).
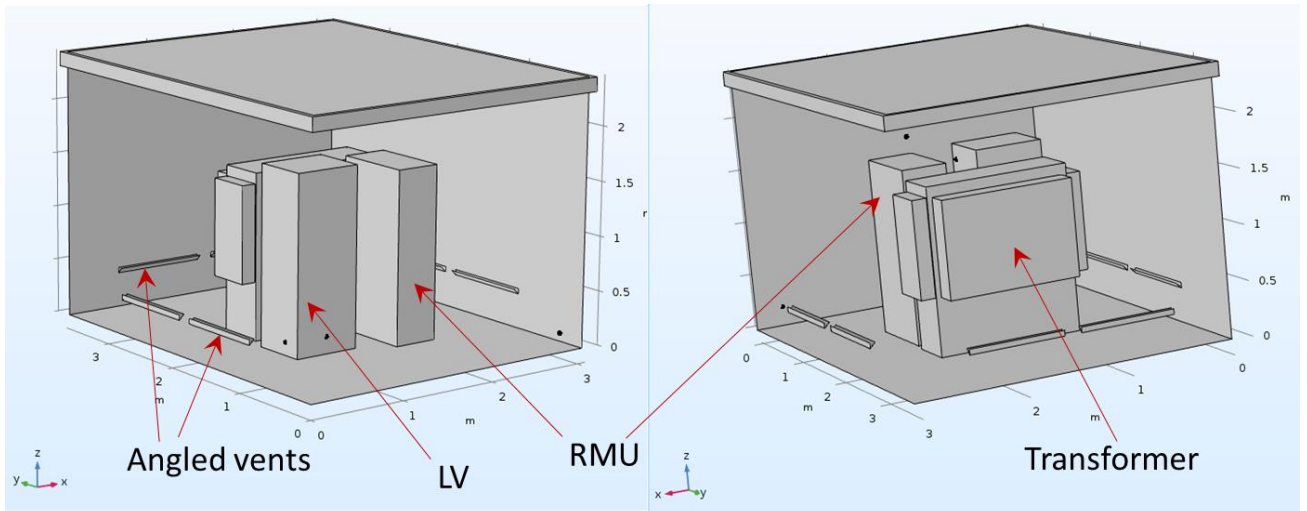
Figure 24: Interior of Southgate Industrial Estate substation from two angles. The roof contains a baffled vent structure as shown in figure 1.
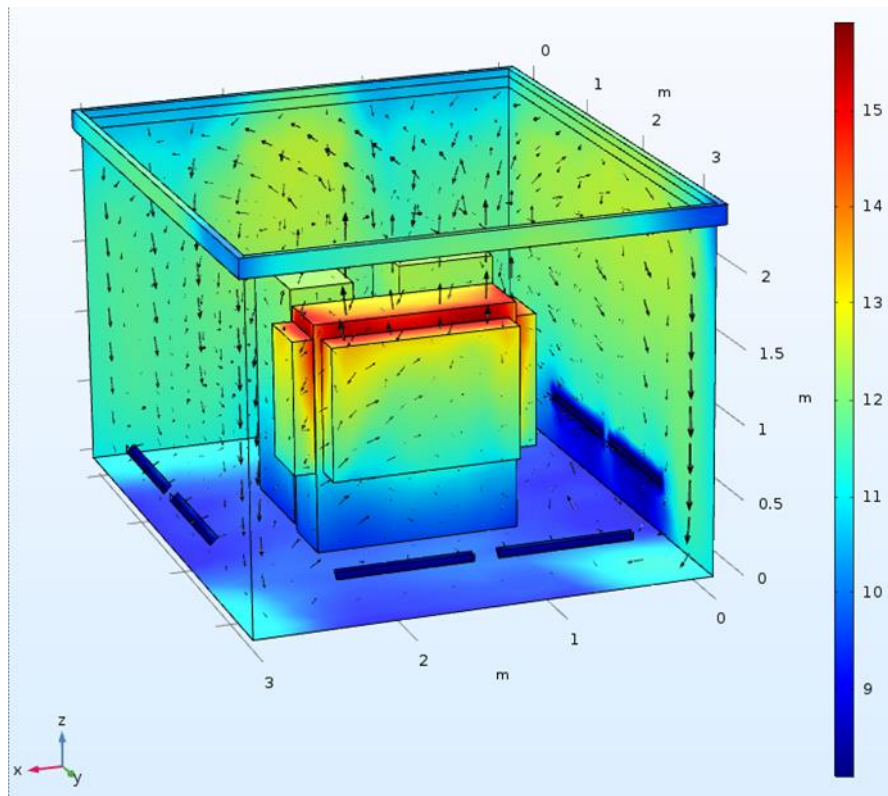

Figure 25: Air flow and temperature distribution within Southgate Industrial Estate.

Figure 26 shows a direct comparison between measured and calculated values. The model over-predicts the temperature low down in the building. The sensor making this measurement was placed close to the corner near the door, which the model predicts to be a location of a downwards flow of hot air. It is possible that any leaks under the door, neglected in the model, could disrupt this flow and disrupt the temperature locally.
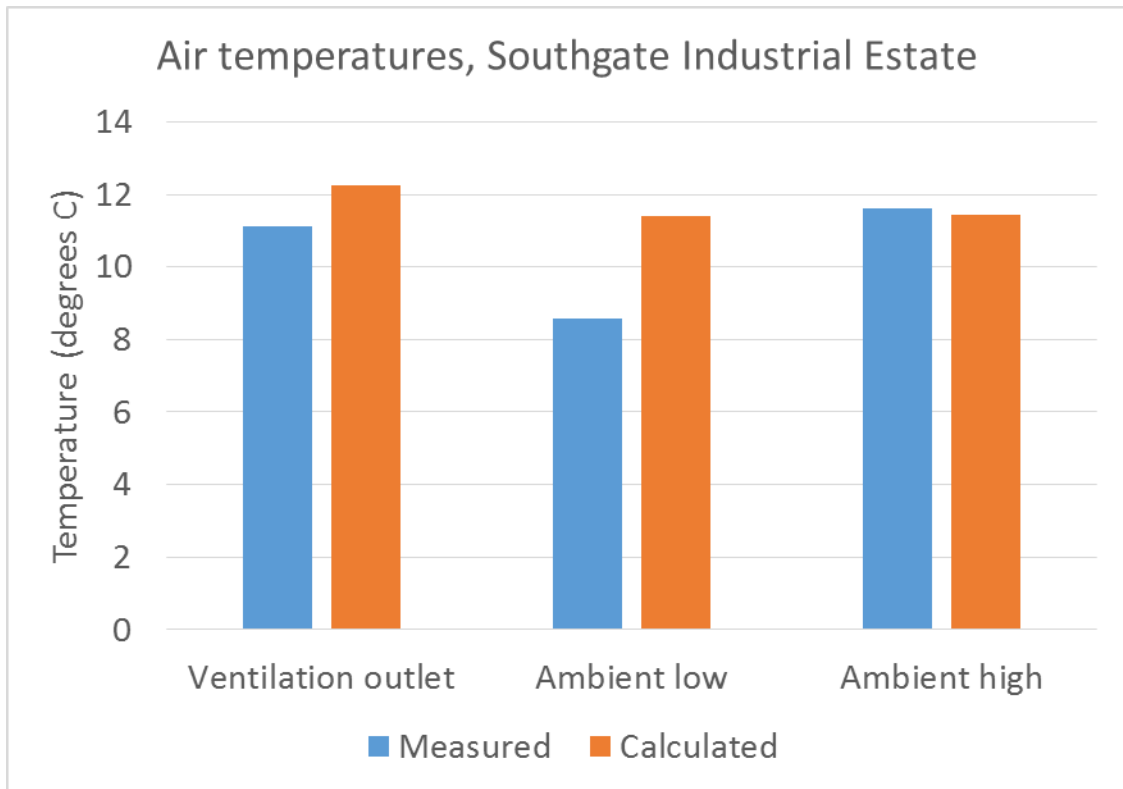
Figure 26: Comparison between measurement and model results for Southgate Industrial Estate.

5.2.5   Town Bridge

Figure 27 shows the location of the objects within the Town Bridge substation. This building is very similar to the Southgate Industrial Estate building, containing a transformer and several cabinets in close proximity. The ventilation is a baffled vent at roof level and a louvred vent low down on every wall, other than that containing the doors.
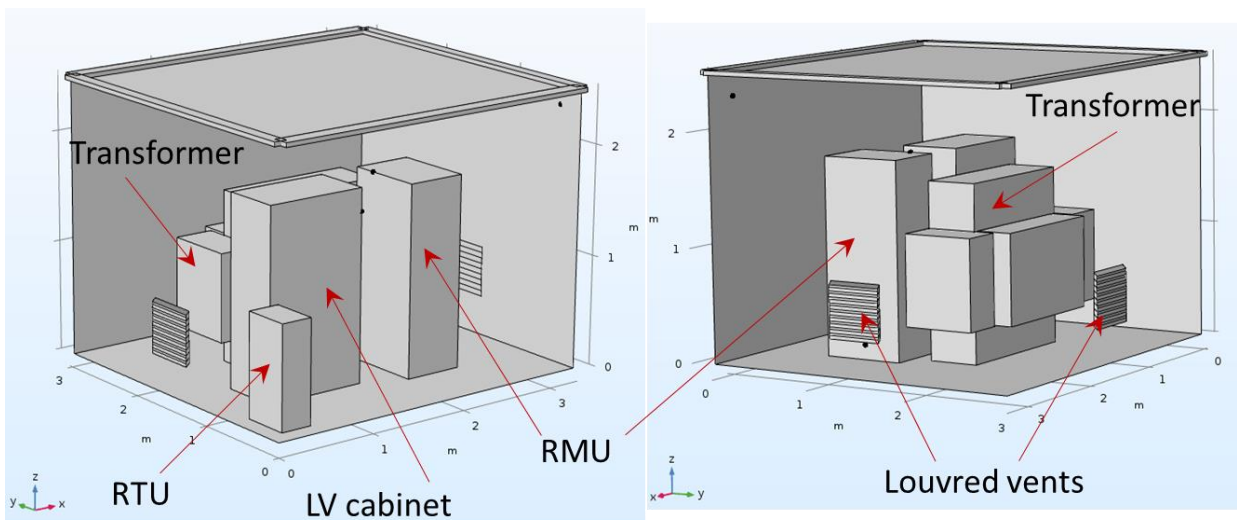

Figure 27: Objects inside the Town Bridge substation from two angles.

Figure 28 shows a plot of the predicted temperature distribution (colour contours) and air flow (arrows show velocity direction, size indicates relative speed) within the Town Bridge model. The plot shows

the flow recirculating within the room, as shown by the arrow directions and the comparatively high temperature of the air next to the walls.
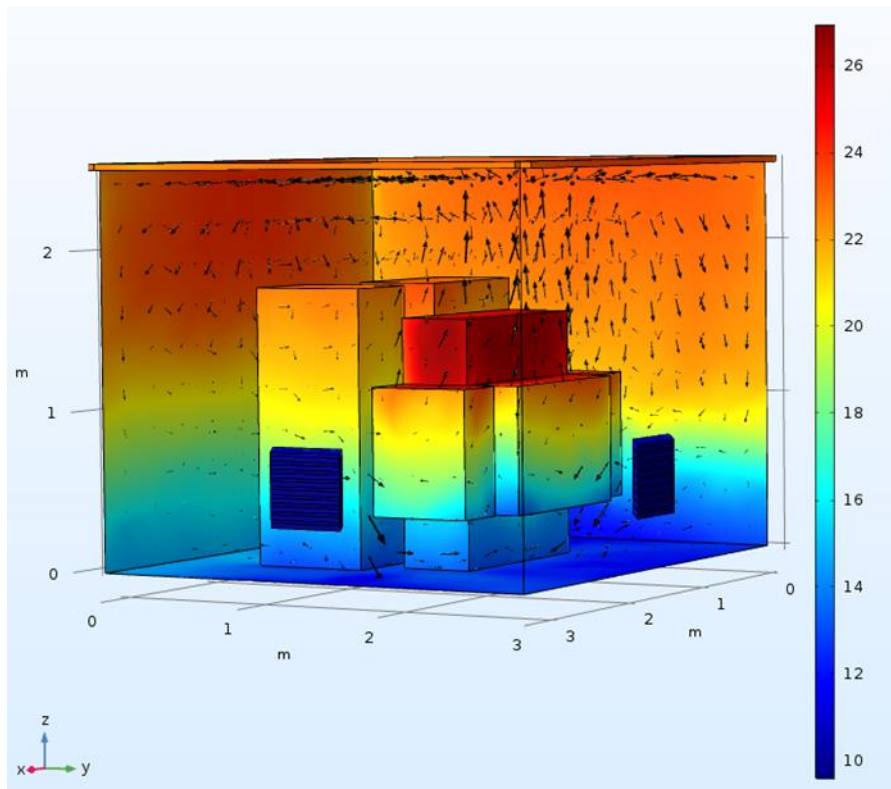

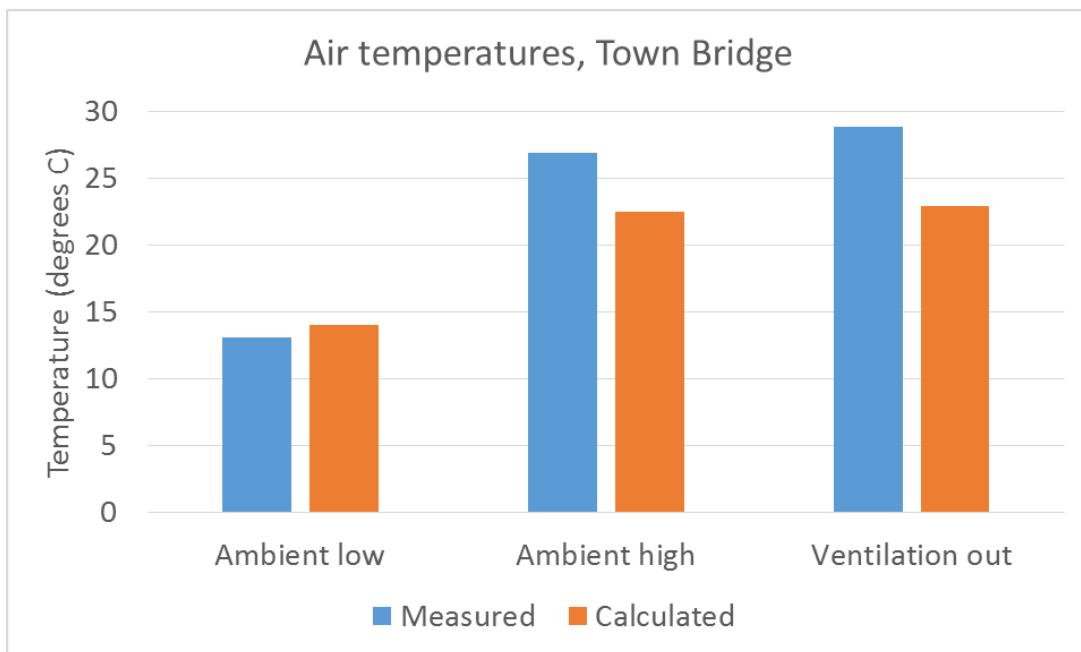**Figure 28: Air flow and temperature distribution within Town Bridge.**

Figure 29: Comparison between measured and calculated air temperatures inside Town Bridge.

Figure 29 shows a direct comparison between the measured and calculated air temperatures in Town Bridge substation. The model under-predicts the temperatures high in the building, by 4 K in one case and 6 K in the other. This under-prediction may be an indication that the model is under-predicting the amount of heat put into the air from the transformer, since the measured temperatures shown are higher than the maximum air temperature predicted by the model.

5.2.6   Wentworth Road

Figure 30 shows the internal details of the Wentworth Road substation. The substation contains HV switchgear and an RTU separated from the transformer, and an LV board adjacent to the transformer. There are two louvred vents at floor level, one close to the transformer, and one vent high up in the wall furthest from the transformer.
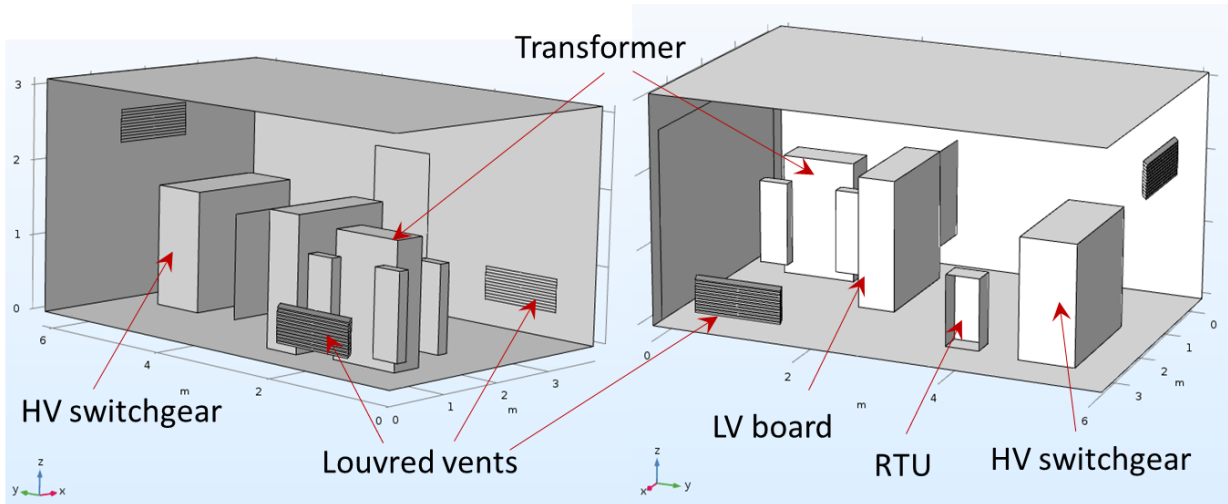

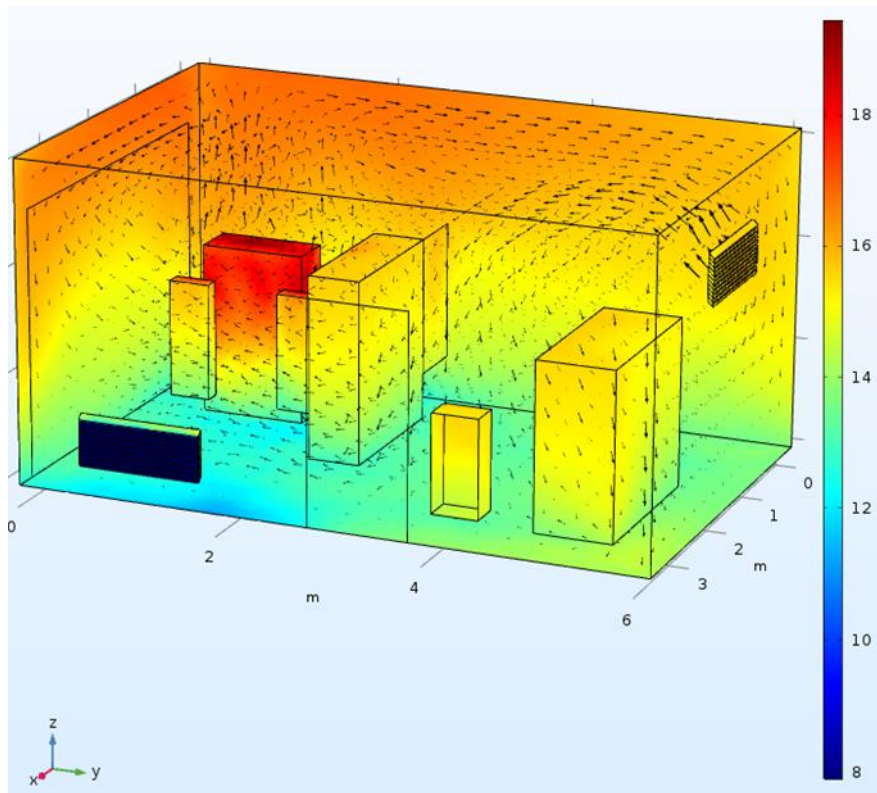**Figure 30: Interior of Wentworth Road substation.**

Figure 31: Air flow and temperature distribution within Wentworth Road.

Figure 31 shows the model predictions of temperature distribution and air flow. The air enters high up and far from the transformer, and leaves through the vents close to the transformer. As a result, the effects of the cold air are diluted and the building is warm.
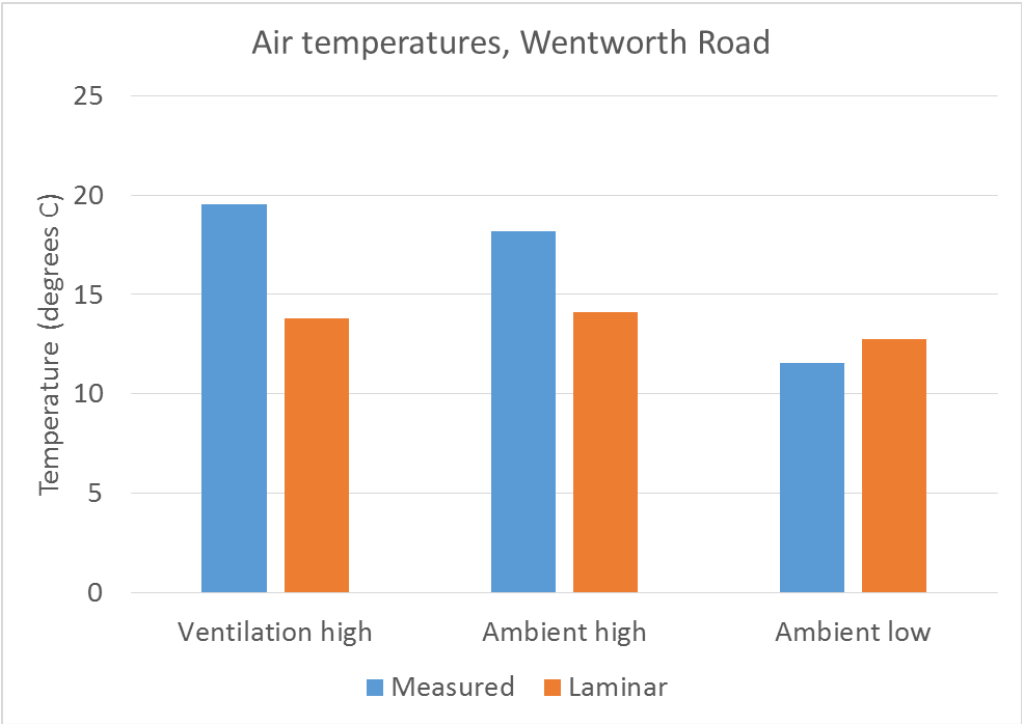

Figure 32: Comparison between measurement and model results for Wentworth Road.

Figure 32 shows the air temperatures measured in Wentworth Road and the equivalent model results. The ventilation high temperature is under-predicted. It is likely that the presence of the HV switchgear cabinet close to the high vent has affected the air temperature there.

6   IMPROVED COOLING AND AIR FLOW

This section provides recommendations for new build and retrofit venting. In most cases these recommendations are based on model results reported above, but in some case extra models have been used to check advice. The recommendations are summarised below and are discussed more generally in the rest of this section.

Recommendations are:

- Where possible, louvred vents should be used in preference to air bricks and should be retrofitted if possible. Vents should be kept clear to encourage airflow.
- Vents should be fitted on more than one wall to avoid an unfavourable wind direction stopping inflow and to get more benefit from favourable winds.
- All vents should be placed as close to the transformer or other significant heat source as other considerations permit, so that the cold air impinges directly on the cooling fins.
- Air should be encouraged to leave the building either by placing a vent directly above the transformer, or by using plates to steer the airflow out of the building.

Note that the recommendations are based solely on thermal considerations: other relevant concerns such as electrical safety, water ingress, etc., have not been taken into account.

6.1 DETAILED DISCUSSIONS

In general, the model results suggest that air bricks do not permit significant air flow into and out of the building and should therefore not be used. Larger louvred vents allow more air flow and should be used where possible.

As a demonstrator, louvred vents of the type used in the Town Bridge model were used to replace the small air bricks in the Portland Grove model. The temperature distribution and air flow pattern are shown in the upper plot of figure 33, and the model results with the smaller vents is shown in the lower plot (a repeat of figure 22). The use of larger vents has decreased the maximum air temperature by about 3 °C, and has increased the power output by the cooling fins from 2017 W to 2414 W.

The results of the wind model (section 4.3) suggested that wind can be a useful source of cooling air, provided that the vent arrangement is such that the in-blown air can leave the building. Vents should therefore be placed on more than one wall.

The model of Wentworth Road with a blocked vent suggested that ensuring the only vents are close to the transformer ensures that the incoming cold air will impinge on the transformer directly rather than being diluted. The colder the air impinging on the transformer cooling fins, the greater the cooling power of the fins.

To test this hypothesis, the Wentworth Road model was reconfigured so that it had two vents directly adjacent to the transformer and no vents anywhere else. A comparison between the temperature and air velocity distributions of the model with the original vent arrangement and the new vent arrangement is shown in figure 34. The two plots in the figure use the same temperature colour scale, so they are directly comparable. This figure shows that the air temperature next to the transformer is lower for the new vent arrangement, because the air impinging on the transformer is at a lower temperature with the new arrangement. The power being lost from the surface of the transformer and its fins was a total of 844 W for the model with the vents close to the transformer, whereas the model with the vents in the existing configuration had a power loss of 794 W, which is considerably lower.
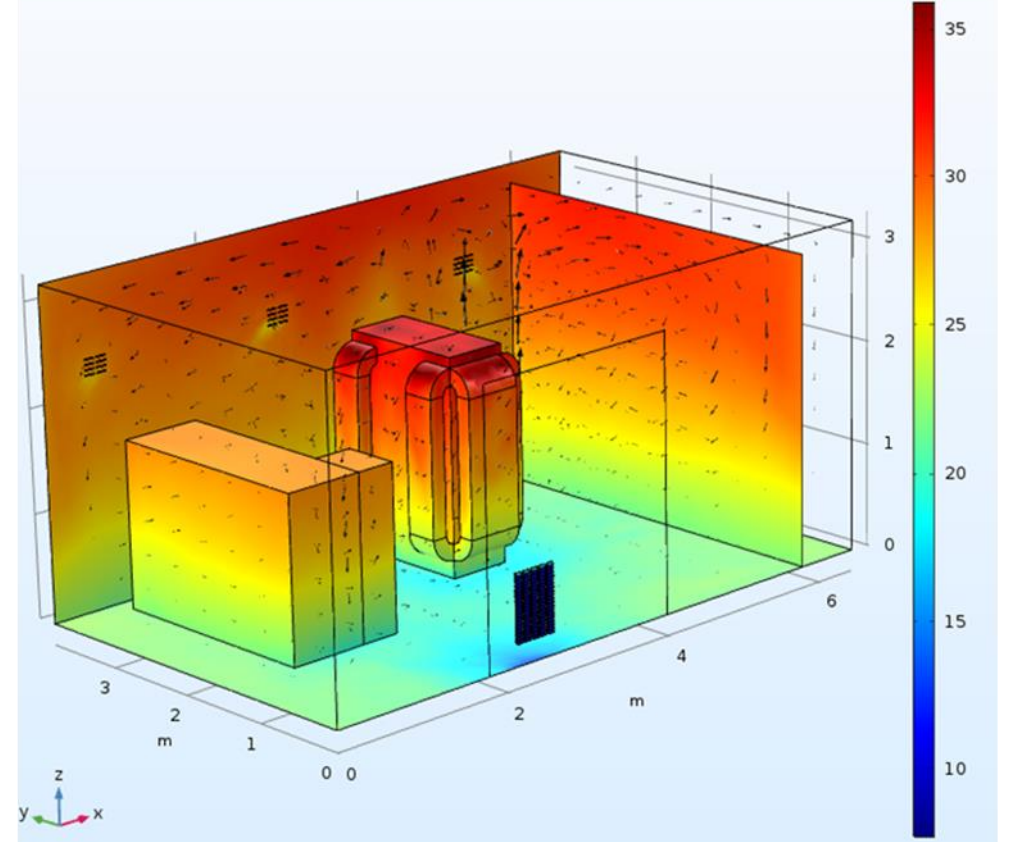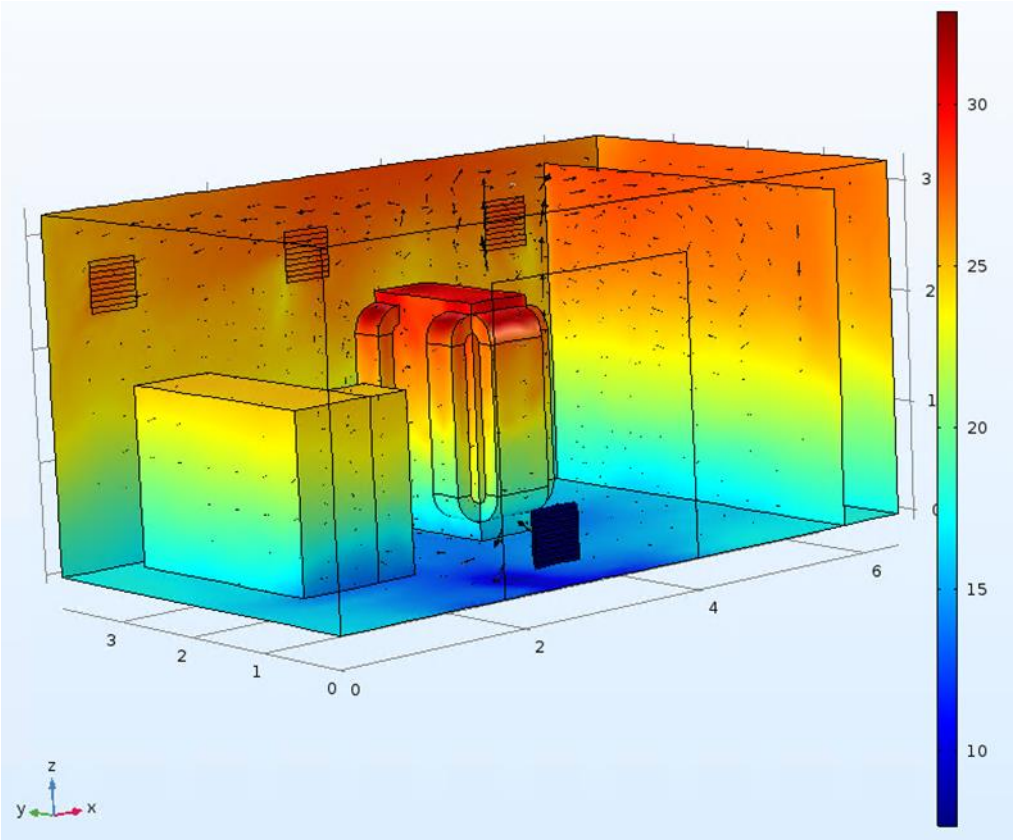
Figure 33: Temperature distribution and air flow pattern in Portland Grove with larger vents (upper plot) and with existing air bricks (lower plot).
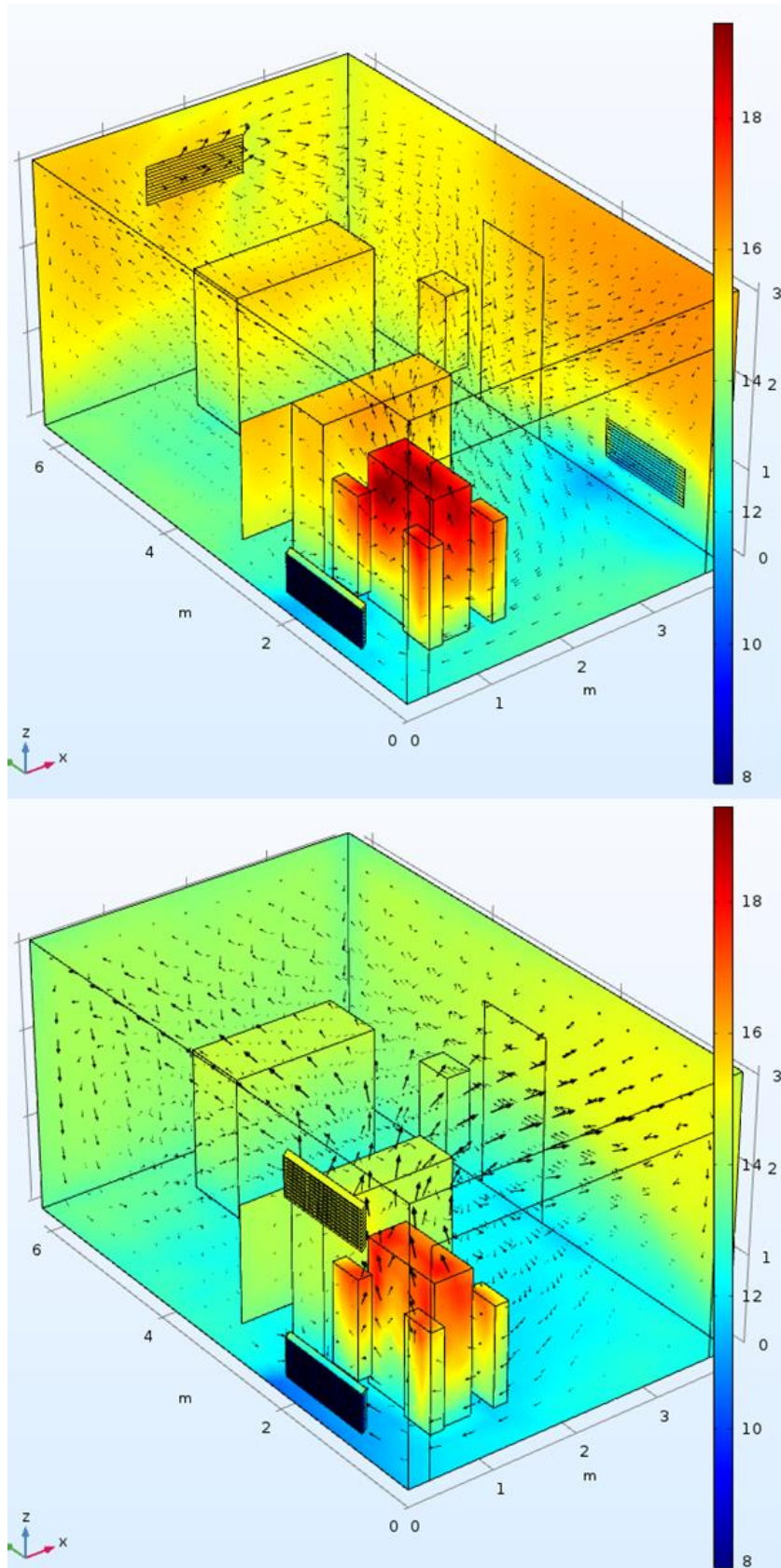
Figure 34: Temperature distribution and air flow pattern in Wentworth Road with the original vent arrangement (upper figure) and vents moved close to the transformer (lower figure).

Most air vent designs depend on pressure differences to get air into and out of buildings, with louvres and vent shaping used externally to stop ingress of rain and windborne detritus. In many cases, this

approach leads to very little air flow in or out of the building so that the air flow is dominated by recirculating flows meaning that the heat transfer out of the building is mostly through the walls and ceiling.

The exception to this situation is the Southgate Industrial Estate building, which has an internal angled section to steer the air out of the building. As a result, the model predicts a higher mass of air entering and leaving the building than other designs.

With this in mind, an extra model was run of the Town Bridge building with an additional vent directly above the transformer. A sketch of the additional vent is provided in figure 35. The presence of the extra vent increased the cooling power of the transformer fins from 2065 W to 2088 W, which is not a huge difference but improved design may be bring further benefits. Figure 36 shows a direct comparison between the temperature distributions with (upper plot) and without (lower plot) the extra vent, which shows no visible difference as would be expected from the small (1 %) change in cooling power. The high temperature of the air in the extra vent suggests that some additional energy is being lost through that route.

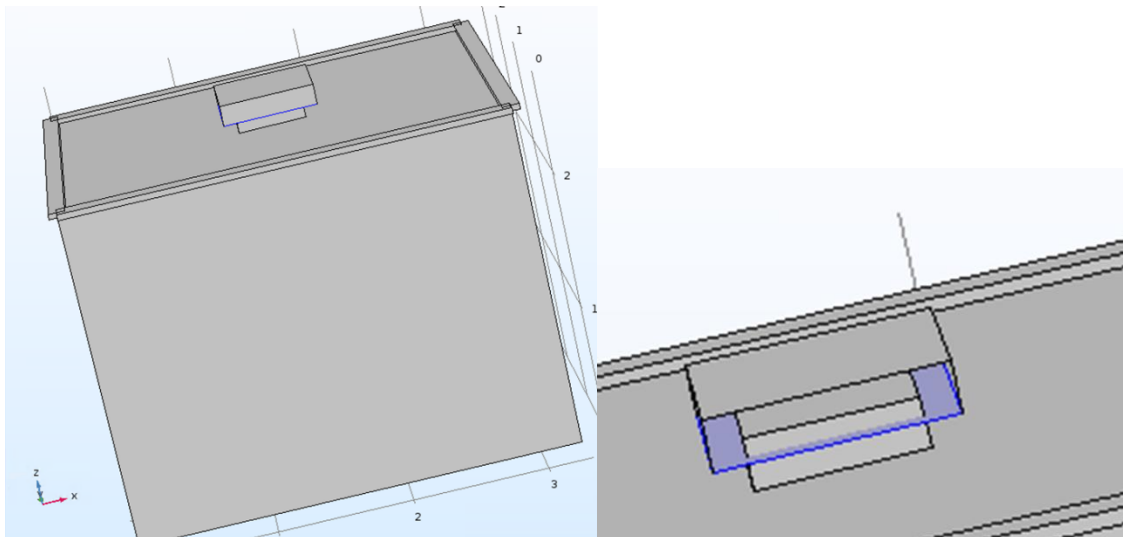More possible designs for air-steering mechanisms will be explored in the next stage of the project.

Figure 35: Extra roof vent in the centre of the Town Bridge building. The figure on the right shows a close-up with part of the wall removed and the region through which air can leave highlighted in blue.
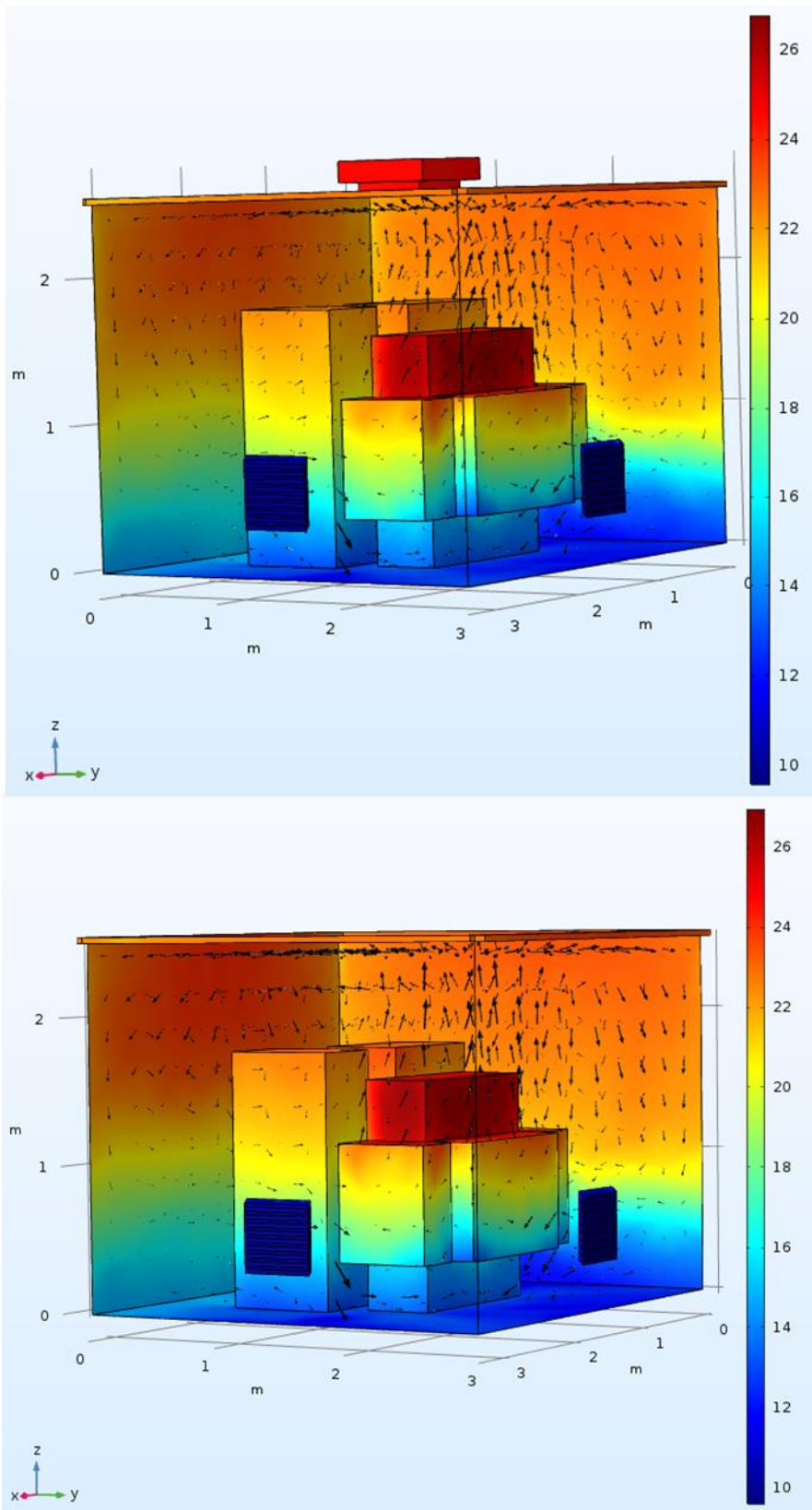
Figure 36: Comparison of predicted temperature distribution within Town Bridge with (upper plot) and without (lower plot) the extra vent.

7   REFERENCES

[1] "Non-stationary thermal model of indoor transformer stations", Radakovic, Z, and Maksimovic, S. Electrical Engineering 84, 109-117, 2002.

[2] "Nonlinear thermal modelling of indoor and outdoor oil-immersed power transformers", Iskender, I, and Mamizadeh, A. Journal of Electrical Engineering, 60(6), 321-327, 2009.

[3] "Evaluation of permissible loading for indoor oil-immersed distribution transformers", Mamizadeh, A, and Iskender, I. Electrical and Electronics Engineering, 10.1109/ELECO.2009.5355332, 2009.

[4] "An improved nonlinear thermal model for MV/LW prefabricated oil-immersed power transformer substations", Iskender, I and Mamizadeh, A. Electrical Engineering, 93(1), 9-22, 2011.

[5] "Analyzing and comparing the hot-spot thermal models of HV/LV prefabricated and outdoor oil-immersed power transformers", Mamizadeh, A, and Iskender, I. International Journal of Electrical, Computer, Energetic, Electronic and Communication Engineering, 6(1), 2012.

[6] "Evaluation and comparing the loss of life for outdoor and MV/LV prefabricated oil immersed power transformer based on nonlinear thermal models", Mamizadeh, A, and Iskender, I. Electrical and Electronics Engineering, 2011. From http://ieeexplore.ieee.org/document/6140218/

[7] "Dynamic Thermal Modeling of MV/LV Prefabricated Substations", Degefa, M Z, Millar R J, Lehtonen M and Hyvönen, P.   IEEE Transactions on Power Delivery, 29(2), 786-793, 2014.

[8] "Numerical modelling of the natural ventilation of underground transformer substations", Ramos, JC, Beiza, M, Gastelurrutia, J, Rivas, A, Anton, R, Larraona, GS, de Miguel, I. Applied Thermal Engineering, 51(1-2), 852-863, DOI: 10.1016/j.applthermaleng.2012.10.032, 2013.

[9] "Zonal thermal model of the ventilation of underground transformer substations: Development and parametric study", Beiza, M; Ramos, JC; Rivas, A; Anton, R; Larraona, GS; Gastelurrutia, J; de Miguel, I. Applied Thermal Engineering, 62(1), 215-228, DOI: 10.1016/j.applthermaleng.2013.09.032, 2014.

[10] "Flow and heat distribution analysis of different transformer sub-stations", Hasini, H, Shuaib, N H, Yogendran, S B, Toh, K B. IOP Conference series: Materials Science & Engineering 50, 012044, 2013.

[11] "Computational simulations and optimization of flow and temperature distributions in a large-scale power plant building", Lee, T, Singh, H, Lee, J, Jeong, H-M, and Sturm, D. Building Simulation, 4(4), 341-349, 2011.

[12] "Computational investigation of ventilation effectiveness in a paper producing industry", Markatos, N C. Drying Technology, 18(9), 2051-2064, 2000.

[13] "Numerical and experimental study of 3D turbulent airflow in a full scale heated ventilated room", Lariani, A, Nesredding, H, Galanis, N. Engineering Applications of Computational Fluid Dynamics, 3(1), 1-14, 2014. Electronic copy not available.

[14] "Validation of measurement techniques and the determination of data required for thermal modelling of moist masonry walls", Williams, R G. Research in Building Physics: Proceedings of the Second International Conference on Building Physics, Leuven, Belgium, 14-18 September 2003.

[15] "Thermal Conductivity and Moisture Measurements on Masonry Materials," Salmon, D R, Williams, R G, and Tye, R P, Insulation Materials: Testing and Applications: 4th Volume, ASTMSTP 1426, A. O. Desjarlais and R. R. Zarr, Eds., ASTM International, West Conshohocken, PA, 2002.

[16] "Evaluation of the thermal performance of insulation systems used in roof structures", Williams, R, Ballard, G. NPL Report MAT8, December 2007.

[17] "Solid wall heat losses and the potential for energy saving. Literature review". BRE report, May 2014. Obtained from https://www.bre.co.uk/filelibrary/pdf/other_pdfs/Solid-wall-insulation-literature-review.pdf

[18] Approved document L1: Conservation of fuel and power. Obtained from http://webarchive.nationalarchives.gov.uk/20151113141044/http://www.planningportal.gov.uk/uploads/br/br_pdf_adl1_2002.pdf

[19] "U-Values of Elements: A guide to the specification of insulation materials in order to achieve compliance with Approved Document L1B 2010 of the Building Regulations for small domestic works", Hertfordshire Technical Forum for Building Control, Technical Note 10, 2011. Obtained from http://www.haringey.gov.uk/sites/haringeygovuk/files/u-value_guidance_nov_06a.pdf

[20] "Research into the thermal performance of traditional brick walls", English Heritage, 2013. Available from https://historicengland.org.uk/images-books/publications/research-thermal-performance-traditional-brick-walls/

[21] "GVA/15 CIBSE Guide A: Environmental Design", Chartered Institution of Building Services Engineers (CIBSE) , 2015.

[22] https://fiberline.com/typical-thermal-properties-fiberline-grp-profiles

[23] https://www.ecfibreglasssupplies.co.uk/topic/glassreinforcedplastics

[24] https://www.travisperkins.co.uk/Hepworth-Red-Square-Hole-Airbrick-215mm/p/867147

[25] http://www.windandsun.co.uk/information/wind-power/info-on-the-uk-windspeed-database.aspx#.Wd-C8KqWx9M

[26] http://www.sussex.ac.uk/weatherstation/technical/Windforce.html